الجمهورية الجزائرية الديمقراطية الشعبية
République algérienne démocratique et populaire
وزارة التعليم العالي والبحث العلمي
Ministère de l'enseignement supérieur et de la recherche scientifique
جامعة عين تموشنت بلحاج بوشعيب
Université –Ain Temouchent- Belhadj Bouchaib
Faculté des Sciences et de la Technologie
Département de Génie Civil et Travaux Publics

Projet de Fin d'Etudes
Pour l'obtention du diplôme de Master en : Structure.
Domaine : Science et Technologie.
Filière : Génie Civil
Spécialité : Structures
Thème

Mathematical modeling and optimization of functionally graded plates

Présenté Par :

1) Melle Nedjadi Ameni
2) Melle Aouggad Bouchera

Devant le jury composé de :

Mr. Amara Khaled	Pr	UAT.B.B (Ain Temouchent)	Président
Mr. Guenanche Boucif	Pr	UAT.B.B (Ain Temouchent)	Examinateur
Mme. Attia Amina	Pr	UAT.B.B (Ain Temouchent)	Encadrant

Année Universitaire 2023/2024

بِسْمِ ٱللَّهِ ٱلرَّحْمَٰنِ ٱلرَّحِيمِ

Acknowledgements

We wish to express our profound gratitude to God, the Almighty and Merciful, who supported us with His strength and patience throughout the completion of this work.

This work was accomplished at the ***Laboratory of Engineering and Sustainable Development*** *at Ain Temouchent University, under the supervision of Dr.* ***Attia Amina****. We would like to express our profound gratitude to her for her encouragement throughout the preparation of this thesis. Her valuable advice greatly helped us in successfully completing this work.*

We are also grateful to the jury members M ***Guenanche*** *and M.* ***AMARA Khaled*** *who kindly agreed to be part of the jury and examine our work.*

A special thank you is dedicated to Mr. ***Bennacer Hamid****, who provided us with the training opportunity.*

Likewise, we thank Professor ***Kadour Hakim*** *for his wise advice and invaluable contribution to the completion of this work. We are grateful for the opportunity to benefit from his experience and knowledge. With all our gratitude.*

Dédicace

A mes plus grand soutiens et sources d'inspiration, je dédie ce travail avec tout mon amour et ma reconnaissance infinis.

*A mes **parents**, je tiens à vous exprimer toute ma gratitude et mon amour pour tout ce que vous avez fait pour moi .votre soutien inconditionnel, vos conseils et votre amour ont façonné la personne que je suis devenu. Vous êtes mes modèles de vie et je suis reconnaissant chaque jour de vous avoir comme parents .merci pour tout que vous avez fait et continuez à faire pour moi .avec amour.*

*A mes frères **Hichem** et **Mohamed**, et à mes chères sœurs **Chaimaa** et **Amina**, qui sont également mes amies proches, merci pour votre soutien continu et votre présence réconfortante. Vous êtes une source de joie et de bonheur pour moi, et je suis fière de vous avoir dans ma vie.*

*A mes chères amies **Azza**, **Fatna**, ma cousine **Sara** et ma cousine germaine **Nour El Houda**, qui ont été mes piliers dans les moments difficiles et mes compagnes de fête dans les moments joyeux, merci pour votre sincérité, votre soutien constant et votre amour inconditionnel.*

*A ma partenaire **Ameni**, qui est devenue une aimée chère et une collaboratrice talentueuse, merci pour notre coopération fructueuse ; et notre amitié, tu as été une source d'inspiration et de motivation tout au long de ce parcours.*

*Enfin, à mon fiancé **Saïd**, mon partenaire de vie et compagnon, merci pour votre soutien constant .tu es ma source de bonheur et je suis reconnaissante tout allèh pour ta présence dans ma vie.*

Bouchera.

Dédicace

J’ai le grand plaisir de dédier ce modeste travail :

À mes très chers parents,

Votre amour inconditionnel, votre soutien et vos encouragements constants. Votre confiance en moi m'a donné la force et la détermination nécessaires pour atteindre mes objectifs. Vous êtes ma source d'inspiration et de motivation améliorée.

À mon chère frère Boualem,

À ma chère sœur Hanadi,

Qui ont toujours été là à mes côtés, me soutenant avec leur amour indéfectible et me souhaitant le meilleur dans la réussite et le bonheur.

À ma grand-mère,

Votre soutien m’a guidé tout au long de ce parcours. Vos histoires, vos conseils et votre sourire réconfortant ont été des piliers inestimables dans ma vie.

À mes oncles et mes tantes

À mes cousine Khadîdja, Meryem, Rym, Siham et Ryhane

À mes cousin Amin, Abd El Djalil, Rayane, Islam, Sofiane, Rabbi, Ibrahim, Adelsamii et Abdelkhalek

Grâce à votre présence à mes côtés, j'ai pu puiser la force nécessaire pour surmonter les défis et persévérer jusqu'à la réussite.

À mes chères amies Fatna , Azza, Amina et Asmaa,

Votre amitié est bien plus qu'une simple compagnie ; elle est un pilier solide sur lequel je me suis appuyée dans les moments de doute et de stress.

À mon cher binôme Bouchera,

Ta force, ta patience et ta compréhension ont été des phares dans les moments sombres. Ton engagement et ton aide précieuse ont été essentiels à la réussite de ce travail.

À tous les membres de ma famille et toute personne porte le nom Nedjadi, Berrichi, Menasra et Sadeddine,

Ameni.

Abstract:

In this study, an overview of functionally graded materials (FGM) was provided, where the first shear deformation theory (FSDT) was used to study the effect of porosity distribution and gradient pattern on the free vibration behavior of functionally graded material plates. The Hamilton's principle was used to derive the motion equations for functionally graded materials plates, using the Navier method for the solution. Through comparison of data from different examples, the accuracy and reliability of the proposed analytical solution were verified. Comparative analysis was also conducted including key parameters obtained in this study.

Keywords: functionally graded materials, first shear deformation theory, porosity, free vibration.

Résumé :

Dans cette étude, une vue d'ensemble des matériaux à gradient fonctionnel (FGM) a été fournie, où la théorie de la première déformation de cisaillement (FSDT) a été utilisée pour étudier l'effet de la distribution de la porosité et du motif de gradient sur le comportement de vibration libre des feuilles de matériaux a gradient fonctionnel. Le principe de Hamilton a été utilisé pour driver les équations de mouvement des feuilles de matériaux à gradient fonctionnel, en utilisant la méthode de Navier pour la solution. En composant les données de diffèrent exemple n l'exactitude et la fiabilité de la solution analytique proposée ont été vérifiées. Une analyse comparative a également été réalisée, incluant des paramètres clés obtenus dans cette étude.

Mots clé : matériaux à gradient fonctionnel, théorie de la première déformation de cisaillement , porosité, vibration libre.

ملخص:

في هذه الدراسة، تم تقديم نظرة عامة عن المواد المتدرجة وظيفيا (MGF)، حيث تم استخدام نظرية الانحناء الأولى لتشوه القص (TDSF) لدراسة تأثير توزيع المسامية ونمط التدرج على سلوك الاهتزاز الحر لصفائح المواد المتدرجة وظيفيا. تم استخدام مبدا هاملتون"(notlimaH)" لاشتقاق معادلات الحركة لصفائح المواد المتدرجة وظيفيا. باستخدام طريقة نافيير"(reivaN)" للحل. من خلال مقرنة البيانات من امثلة مختلفة، تم التحقق من دقة وموثوقية الحل التحليلي المقترح. كما تم اجراء تحليل مقارنات يشمل معلمات رئيسية، المحصل عليها من هذه الدراسة.

الكلمات المفتاحية: المواد المتدرجة وظيفيا -نظرية الانحناء لتشوه القص من الدرجة الأولى-المسامية - الاهتزاز الحر.

Table of contents

List of figures

Chapter I. Functionality graded materials

Chapter II. Theories of plates

Chapter III. FGM of plates

Chapter IV. Results and discussion

List of tables

Chapter I. Functionality graded materials

Chapter IV. Results and discussion

List of grades

FGM	: Functionally graded material
P-FGM	: Power-low functionally graded material
E-FGM	: Exponential-law functionally graded material
S-FGM	: Sigmoid-law functionally graded material
CPT	: Classical plate theory
FSDT	: First-order shear deformation theory
HSDT	: Higher-order shear deformation theory
FEM	: Finite element method
SCF	: Shear correction factor
C	: Ceramic
M	: Metal
P	: Elasticity modulus
E	: Young's modulus
a	: Length of plate
b	: Width of plate
h	: Thickness of plate
p	: Gradient index
z	: Vector thickness
u	: In-plan transverse displacement of the x-axis
v	: In-plan transverse displacement of the y-axis
w	: In-plan transverse displacement of the z-axis
λ_0	: Porosity
k_s	: Shear correction coefficient
N	: Axial force resultant

Q : Shear force resultant

M : Moment resultant

I : Mass moment of inertia

ω : Non-dimensional frequency

a/h : Width-to-thickness

$\emptyset_x$: Rotational displacement components of the x-axis

$\emptyset_y$: Rotational displacement components of the x-axis

ε : Normal strain

γ : Shear strain

$U_{mn}, V_{mn}, W_{mn}, X_{mn}, W_{mn}$: Mass moment of inertia

A, B, C, D : Four different porosity distributions

General Introduction

Due to rapid advancements in material science, functionally graded materials (FGMs) are supplanting conventional materials in high-performance engineering sectors such as aerospace, marine technology, and automotive manufacturing. Japanese scientists have significantly contributed to expediting these transformations through their advanced research, development, and application of functionally classified materials.

Their work has led to the creation of new materials with specific characteristics, resulting in improved power and performance, even in challenging conditions (M.Koizumi, 1993). Previously, the production of engineering materials aimed to achieve homogeneous qualities, ensuring minimal variations in their characteristics after use and enabling them to offer the best possible performance for various industrial applications. However, thanks to advances in materials science, a new paradigm has been established by favoring the production of materials with specialized characteristics to meet specific performance requirements in different industries (Saleh, 2020).

Many researchers have been interested in studying the bending, free vibration, dynamic response, and buckling characteristics of beams, plates, and shells made of functionally graded materials (N.D.Duc, 2014). The academic literature has shown great interest in the use of various theoretical techniques in studying functionally graded material (FGM) plates. These include the traditional plate theory (CPT), the first-order shear deformation theory (FSDT), and the higher-order shear deformation theory (HSDT). Researchers can employ different tools to study the complex characteristics and responses exhibited by FGM plates, leveraging these concepts (Nguyen, 2019).

Several researchers have been interested in studying the bending, free vibration, dynamic response, and buckling characteristics of beams, plates, and shells made of functionally graded materials. For example, (Abrate, 2008) A thorough study was conducted by (Abrate, 2008) et al on the free vibration of a simply supported rectangular FGM plate. To calculate the frequency values of the FGM plate under various boundary conditions, (Chakraverty, 2014) employed the Rayleigh-Ritz method, referring to the principle of the classical plate theory (CPT). By using geometric analysis and non-uniform rational B-splines,(Yin, 2013) conducts vibration studies, reducing memory usage and improving efficiency. Furthermore, (Hosseini-Hashemi, 2011) employed Mindlin plate theory to derive an accurate solution for the three-dimensional vibration of medium-thick FGM plates. The new FSDT was employed to study the bending and vibration characteristics of FGM plates in order to analyze their behavior (Thai, 2013).

According to (Jrad, 2019), a geometric nonlinear analysis of FGM shell structures was conducted using FSDT. In their study, (Valizadeh, 2013) at al examined the various properties of FGM plates using FSDT based on the isogeometric finite element method using NURBS. To evaluate the vibration performance of FGM plates with variable and uniform thicknesses, (Kumar, 2023) et al employed FSDT and the dynamic stiffness method. (Liu, 2016) et al employed the layerwise theory and finite element method to analyze the free vibration of functionally graded material sandwich shells. The results revealed accurate solutions for various functionally graded material shell structures.

(Parida, 2020) employed the meshless local Petrov-Galerkin method to investigate the free and forced vibrations of FGM plates by integrating the Higher-order Shear Deformation Theory (HSDT) and the theory of normal deformed plates. This was carried out using the multiquadric radial basis function method associated with the HSDT, the free vibration of FGM plates was studied by (C. M.C. Roque, 2007) under various boundary conditions. According to (Liu, 2016), isogeometric analysis was employed to study the behavior of free vibration.

According to (Aydogdu, 2007), higher-order deformation theories can be developed based on assumptions about the variation of axial displacement through the thickness of the beam, considering either axial displacements alone or both axial displacements and transverse deformation through the thickness of the beam.

In recent years, the study of various porous FGM structures, whether uniform or not, with varying porosity distributions, has garnered increasing attention. (Thanh, 2020) and (Cuong-Le, 2022) conducted a detailed parametric analysis of the static and dynamic behavior of porous FGM plate structures. The study of the influence of porosity on the critical force and crack path of FGM structures was conducted using isogeometric analysis. Additionally, the first-order shear deformation theory (FSDT) was employed to analyze the nonlinear dynamic response of composite sandwich shallow spherical shells reinforced with graphene platelets with porosity (Anh, 2021).

According to (M. Kaddari, 2020), natural oscillations are observed in porous plates made of functionally graded materials (FGM). Furthermore, a study was conducted on the dynamic response of sandwich structures consisting of porous panels with various reinforcements. The nonlinear Coupled Perturbation Theory (CPT) was used to analyze the large-amplitude vibrations of porous plates made of FGM materials with a sigmoid composition (Zu, 2017). Using the First-order Shear Deformation Theory (FSDT). In his study, (Kumar, 2023) investigated the nonlinear free vibrations of inclined porous FGM plates, considering variations

in porosity and distribution. Furthermore, he employed the FSDT to delve deeper into the vibrational properties of porous conical FGM plates and proposed analytical solutions that include various material asymptotic functions and porosity distributions.

After analyzing the above literature, we noticed that there were few studies that examined the joint influence of distribution type and grading pattern on the response of porous FGM structures. Furthermore, not enough attention has been paid to the complex relationship between these factors.

This thesis is structured into four parts, as follows: Once a general introduction has been given to functionally graded materials, also known as materials with graded properties or functionally graded materials, and the thematic framework has been established for this thesis.

- The first chapter presents a bibliographic study of composite materials, focusing on their benefits and uses in various industries. It also includes detailed information on the properties of functionally graded materials (FGM).
- In Chapter II, a bibliographic review of the various plate theories used was presented.
- Chapter III focuses on presenting the effect of porosity distribution shape on the mechanical behavior of FGM plates using FSDT (First-order Shear Deformation Theory).
- The fourth chapter includes validation and comparison of the results.

The study will end with a conclusion about this work and potential directions for the future.

Chapter I. functionally graded materials

I.1 Introduction

The search for materials with practical benefits like light weight, strong chemical and mechanical resistance, high durability, low maintenance, and shortened manufacturing times is at the heart of modern technology. Recent developments in materials science have had a significant impact on how technology is shaped. Scholars are investigating inventive approaches, utilizing composite materials to attain unparalleled characteristics concerning durability, pliability, and eco-friendliness. This endeavor not only transforms established sectors but also opens doors for innovations in developing areas such as wearable technology, renewable energy, and smart infrastructure.

Within the field of contemporary technology. Through interdisciplinary research, multifunctional materials that adapt to different environments and provide adaptive solutions are developed to new heights.

The qualities and attributes of each kind of substance depend on its class. Although metals are often ductile, they often have a high density. Lightweight polymers can also be fragile, have low mechanical properties, and reduced stiffness. However, ceramics are brittle by nature despite having extremely high tensile strength and Young's modulus. When multiple kinds of ordinarily immiscible materials are combined while maintaining control over their shape and distribution, composite materials are created that have characteristics entirely distinct from those of their constituent parts. This method has been around for ages.

It is clear that the advancement of contemporary technologies required the employment of materials with low volumetric masses but particular high mechanical qualities appropriate for their intended use. In particular, reducing the bulk of the buildings is the objective. Materials that satisfy these requirements are known as composite materials. Originally used for a variety of structural components, particularly in airplanes, composite materials were chosen for their low density, high strength, notable stiffness, and exceptional longevity.

The development of composite materials has made it possible to combine specific properties with different materials within the same part. The local optimization of these properties, by association of a high-hardness material with the surface of a tough material, for example, then poses the problem of the interface. This sudden transition of compositions can locally generate high stress concentrations. The solution of a continuous transition of the desired

properties by a composition gradient makes it possible to attenuate this singularity through the use of functionally graded material. “F.G.M” (ziou, 2017).

I.2 The composites materials:

The idea of "composites" was not created by humans. Wood is a naturally occurring composite material made of one type of polymer, stiff and strong cellulose fibers, encased in a resinous matrix of another polymer, the polysaccharide lignin. composite material is generally made up of one or more discontinuous phases divided into a continuous phase. In general terms, the discontinuous phase has stronger mechanical properties than the continuous phase. “The reinforcing” designates the phase to discontinue and “the matrix” the phase to continue (Harris, 1999)**.**

At the moment, materials with strong fibers, whether continuous or not, are referred to as composite materials. embedded in a matrix or weaker substance. The matrix transfers the load operating on the composite component to this fiber while maintaining the fibers' geometric arrangement (Gay, 2022).

A composite material made up, generally, of one or more phases that are discontinuous divided into a continuous phase. In general terms, the discontinuous phase has stronger mechanical properties than the continuous phase. “The reinforcing” designates the phase to discontinue and “the matrix” the phase to continue (ziou, 2017).

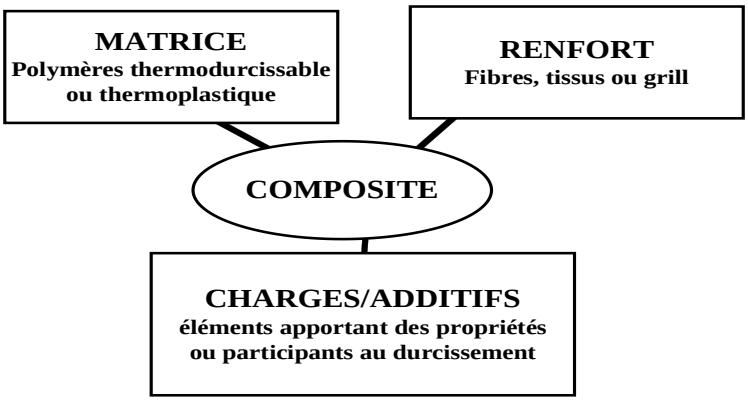

Figure I. 1 : Composite materials

The reinforcement phase, which frequently takes the form of fibers or particles, adds to the overall mechanical properties of composite materials, including stiffness and tensile strength.

Conversely, the matrix phase—usually a polymer resin—transfers load, binds the reinforcement together, and shields it from the elements, including moisture and corrosion. Reinforcement and matrix work together to give composites qualities that are better than those of their basic parts. The intended performance requirements of the composite and the application conditions it will face determine the choice of reinforcing and matrix materials. Thus, to maximize the qualities of the composite and guarantee its efficacy in practical applications, one must comprehend the interplay between the matrix and reinforcement.

I.2.1 Definition of reinforcing :

Reinforcement of composite materials is the main component supporting mechanical action. It can represent different forms

- Special goods in the form of microplates, Broy fibers, micron or nanoparticle powders.

- Fibrous materials for matt, unstructured surfaces,
- Fibers are made up of the fabric or unidirectional fabric that makes up the blanket (BRAIRI, 2019).

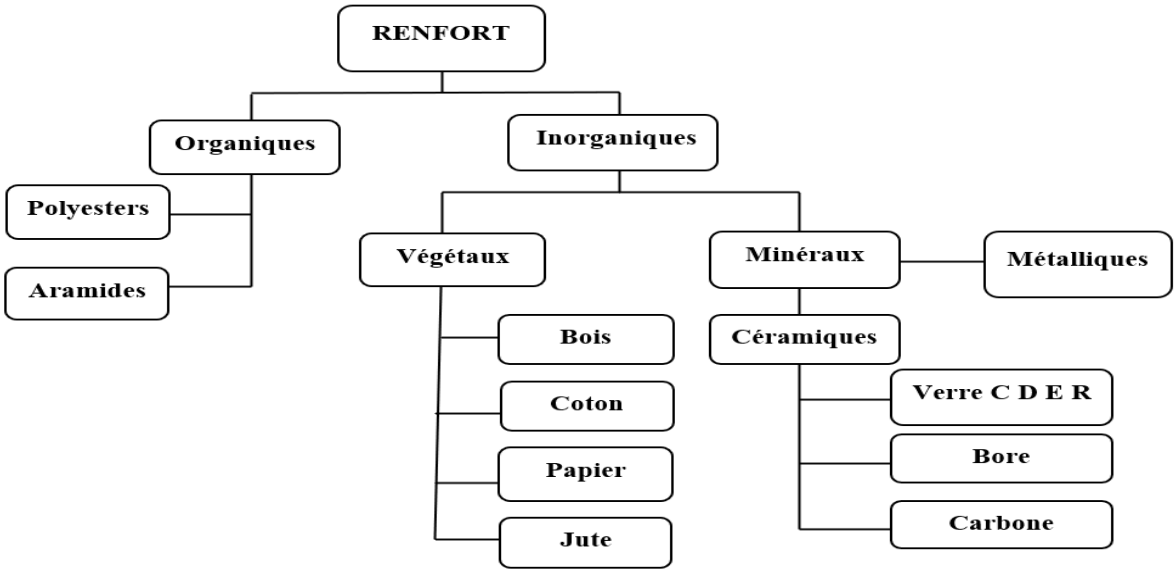

Figure I. 2 : Reinforcement families

I.2.2 Definition of matrix:

The most important goal of the matrix is to transmit mechanical force.

Ranford. It also ensures the protection of the reinforcing in different conditions. Environment (oxidation, moisture loss, corrosion, etc.). On Distinguishing the Three-Body Problem.

- Thermoplastic resins;
- Thermoplastics
- Elastomers (BRAIRI, 2019).

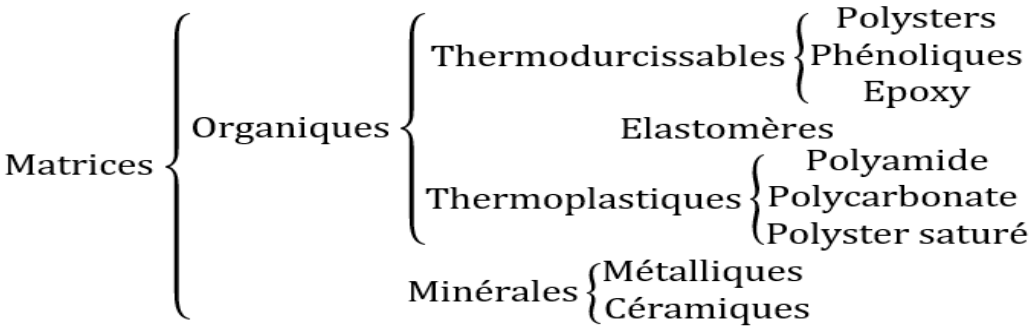

Figure I. 3 : Families of matrix

I.3 Functionally grade materials :

I.3.1 The history of graded functionally materials :

The idea of functionally gradient materials (FGM) was first introduced in Japan in 1984 as part of a spacecraft project. His goal was to develop materials that could function as thermal barriers in extreme situations, such as 2000 K surface temperatures and 1000 K temperature gradients across a 10 mm length. This novel approach has garnered attention on a global scale, sparking increased interest and research activities, particularly in Europe and Germany.

Germany has developed into a significant hub for FGM research and development in recent years. The establishment of a Center for Collaborative Transregional Research (SFB Transregio) in 2006 is evidence of the nation's commitment to investigating the potential of FGM. This center focuses on using nanomaterials, such as aluminum, polypropylene, and steel,

in thermomechanical coupled fabrication processes to create advanced flexible glass moldings with improved performance characteristics and adjustable properties. This multidisciplinary approach brings together specialists from several fields to foster innovation and address the significant engineering challenges related to the manufacture and use of FGM (Randjbaran, 2015).

I.3.2 Definition :

The capacity of functionally graded materials (FGMs) to adapt to hostile conditions without sacrificing structural integrity gives them a unique edge in engineering applications. FGMs show a progressive transition in composition from one material to another, which is different from ordinary composite materials and enables tailored properties throughout the material's volume. FGMs may accomplish a wide range of functions thanks to their compositional gradient, which makes them extremely adaptable in a variety of engineering applications.

FGMs are an example of a biomimetic approach to material design, drawing inspiration from nature, where intricate structures frequently maximize functionality. Engineers try to create materials that can better endure dynamic and demanding environments by imitating natural gradients and compositions.

Research on the modeling and optimization of FGM structures has drawn attention from both scientists and engineers. Researchers aim to predict and improve the mechanical behavior of FGMs through sophisticated computational methods and experimental validation, facilitating the construction of more robust and effective structures for a variety of applications.

To sum up, FGMs represent a promising approach to tackling engineering problems and expanding the limits of structural performance and durability. They are at the forefront of materials research (mahamood, 2017)

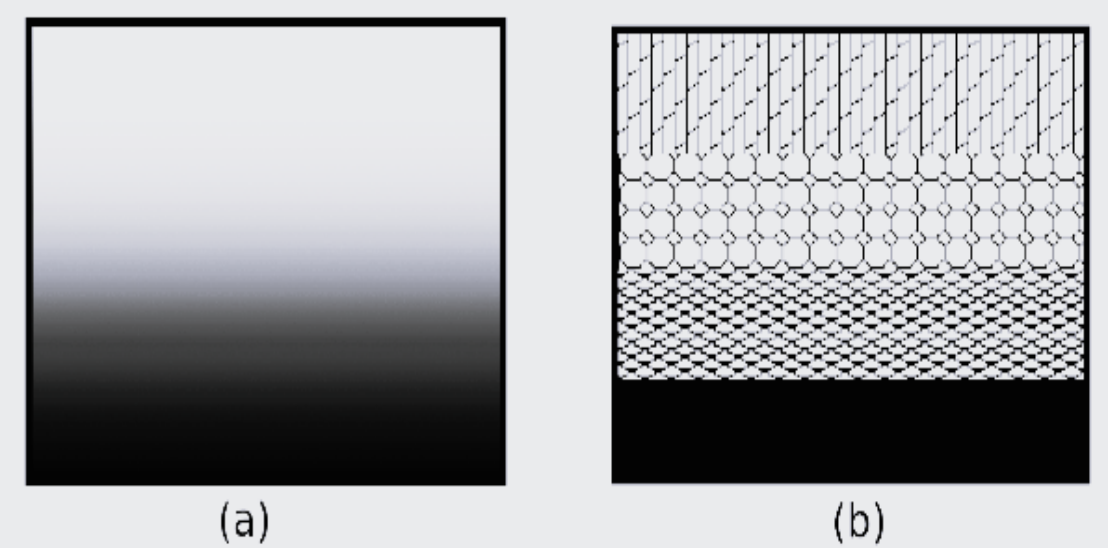

Figure I. 4 : variation of (FGM)

(a)variation continue, (b)variation discontinue

I.3.3 Characteristics of FGM materials:

The special composition of gradient functional materials (FGM), which consists of both metal and ceramic phases with continuous composition fluctuation, contributes to their remarkable qualities. Unlike conventional composite materials, fiber glass mats (FGM) exhibit seamless transitions between phases, allowing for the optimal utilization of each constituent material's advantageous properties (AIT FERHAT, 2021).

This two-phase composition enables FGM to express a combination of desired characteristics, such as high resistance to the temperatures of the metal phase and thermal conductivity of the ceramic phase. Because of their polyvalence, FGM are well suited to a wide range of industrial applications where the ability to function in extreme environments is essential.

The unique qualities of FGM make them more and more appealing for use in the aerospace, automotive, and energy sectors, among other industries, as they search for materials that can withstand harsh environments without losing their structural integrity. Current research and development on FGM aim to further unlock its potential and expand its uses across several fields.

Because FGM are composite in nature, with constant changes in composition and microstructure, they exhibit macroscopical heterogeneity. This gradient establishes the special qualities of FGM materials that enable them to adjust to changing mechanical requirements as

well as environmental circumstances. Interestingly, FGM can have different microstructures while maintaining the same material composition, highlighting the versatility and complexity of these designed materials (Abdelouahed Tounsi, 2013).

Table I. 1: Characteristics of the different layers of FGM materials

Couches	**Materials**	**Mechanical Properties**
The high Temperature face	Ceramic	– Good thermal resistance – Good resistance to oxidation – Low thermal conductivity
≪ Middle layer ≫ Continuity of the material from one point to another	Ceramic−metal	– Elimination of interface problems – Relax thermal constraints
The face based on temperature	Metal	– Bonne mechanical resistance – High thermal conductivity – Very good tenacity

Table I. 2: Characteristics of FGM and their important application

Sl. No	FGCM Type	Requirement	Application
1	Al / Sic	Hardness & $Toughness$	-Combustion chambers
2	Al / C	–	-Drive shaft, Turbine -Rotors, Turbine Wheels
3	Si C / Sic	Corrosion Resistance And hardness	-Combustion chambers
4	Al / Sic	–	-Fly wheels, Racing Car Brakes
5	$Al_2\ O_3$ / Al $-alloy$	Good Thermal & corrosion resistance	-Rocket Nozzle, wings, Rotary Launchers, Engine casing

I.3.4 Advantages and disadvantages of FGM and its application areas:

Like any other material, FGM has advantages and disadvantages that we will list below for its application. We will outline the fields in which FGM finds application and provide a few instances of its use in the field of civil engineering.

Advances in FGM:

- When used as an interface layer to join two incompatible materials, FGM can significantly strengthen the bond.
- One possible use for the FGM interface and covering is to lessen thermal and residual resistance.
- The FGM material has the ability to regulate deformation, dynamic response, usure, corrosion, etc.
- The FGM also provides the opportunity to benefit from many material kinds, such as metals and ceramics (Guellil, 2022).

Consequences de la FGM:

- Further research and a more thorough examination of the material model's physical properties are still required.
- Production expenses are still very high.

FGM is characterized by a wide range of applications. Notable among them are building materials, energy conversion materials, aerospace, space, nuclear, and semi-conductor materials. Thus, these materials have two opposing properties: thermal conductivity and thermal isolation. Indeed, they enable the fabrication of lightweight, resilient, and long-lasting materials.

Thermal Management

- Thermal barrier coatings on engine components.
- Heat sinks for electronic devices
- Thermal insulation in aerospace applications

Tribology (Wear and Friction)

- Gradient coatings for cutting tools and wear-resistant surfaces
- Bearing materials with improved lubricity and wear resistance
- Brake linings with enhanced friction and wear properties

Corrosion Resistance

- Protective coatings on pipes, vessels, and structures
- Biomedical implants with corrosion-resistant surfaces
- Marine structures with improved durability

Optoelectronics

- Optical filters and anti-reflection coatings
- Lenses and waveguide devices with tailored optical properties
- Light-emitting diodes (LEDs) with enhanced efficiency

Biomedical Engineering

- Tissue scaffolds with tailored mechanical and biological properties
- Drug delivery systems with controlled release rates
- Dental prosthetics with graded stiffness and wear resistance

Aerospace Engineering

- Lightweight and strong materials for aircraft structures
- Thermal protection systems for spacecraft
- Electromagnetic shielding materials for electronic systems

Automotive Industry

- Lightweight and durable components for body frames
- Catalytic converters with improved efficiency

- Fuel injection systems with enhanced precision

Other Applications

- Piezoelectric sensors and actuators
- Energy storage materials
- Sensors for harsh environments

I.4 Comparative analysis of FGM and composite materials :

Functionally graded materials (FGMs) are composed of many layers containing different elements such as metals and ceramics. These composite materials' macroscopically inhomogeneous characteristics allow for customized performance in various areas of the material because they vary depending on where they are located.

FGMs are different from traditional composite materials in that their composition is constantly changing, which affects the material's microstructure. While the constituents of conventional composites are often mixed uniformly or layered differently, the transition between the various elements occurs gradually and continuously in FGMs. For certain applications, the material's mechanical, thermal, and other properties can be optimized thanks to this progressive fluctuation. FGMs have distinct advantages over conventional composite materials due to their regulated gradation of composition and qualities.

Figure I. 6 established a basic model difference in compositions and properties between an ordinary composite material and FGM. There is a distinct interface between metals and ceramics in an ordinary composite material, but not in an FGM. This difference corresponds to the distribution of properties such as thermal expansion coefficient, thermal conductivity, and thermal resistance. An ordinary composite material contains a sudden change in properties at the interface, while an FGM presents a gradual change inside it. The difference in thermal expansion coefficients at the interface causes internal thermal stress at elevated temperatures, sometimes leading to the destruction of the interfaces. As shown in Figure, an FGM reduces thermal stress by almost 30% and can prevent destruction of the interface (SOMIYA, 2013).

I.5 Laws governing the change in the material properties of FGMs:

In order to maximize the performance of the structure they comprise, FGM property gradient materials combine two materials with distinct structural and functional qualities. The transition between these materials should ideally be continuous in terms of composition, structure, and porosity distribution. The difference in volume fractions can be used to characterize a FGM.

When describing volume fractions, most researchers choose the sigmoid, exponential, or power functions. The particle-to-particle bonds need to be strong enough from the inside to resist rupture and from the outside to stop wear (Z, 2016).

These materials are perfect for applications where there are high temperature variations because of their exceptional resistance to thermal stresses. Furthermore, FGMs can be designed to offer a progressive shift in thermal expansion coefficients, which lowers the possibility of delamination and improves structural integrity. Additionally, they have enhanced load-bearing capacities, which are crucial in industries like aerospace and military. Innovative solutions in cutting-edge engineering and manufacturing processes are made possible by the ability to customize FGMs for certain mechanical and thermal properties. Additionally, FGMs are being investigated more and more for biomedical applications where material performance and compatibility is crucial, including implants and prostheses.

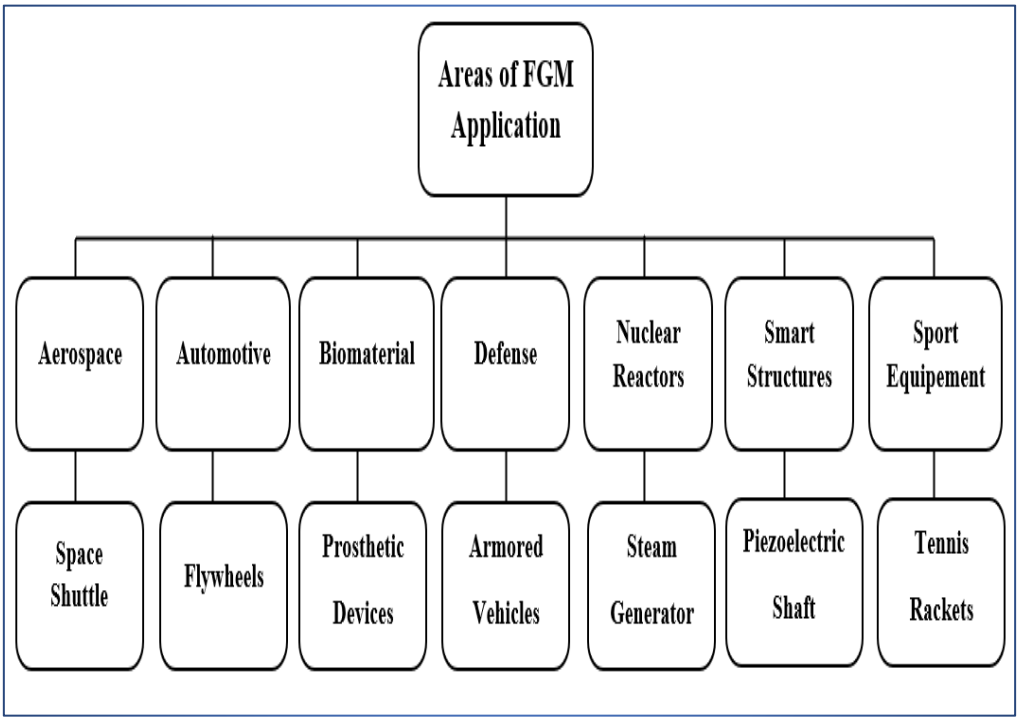

Figure I. 5 : Multiple areas in which FGM is used

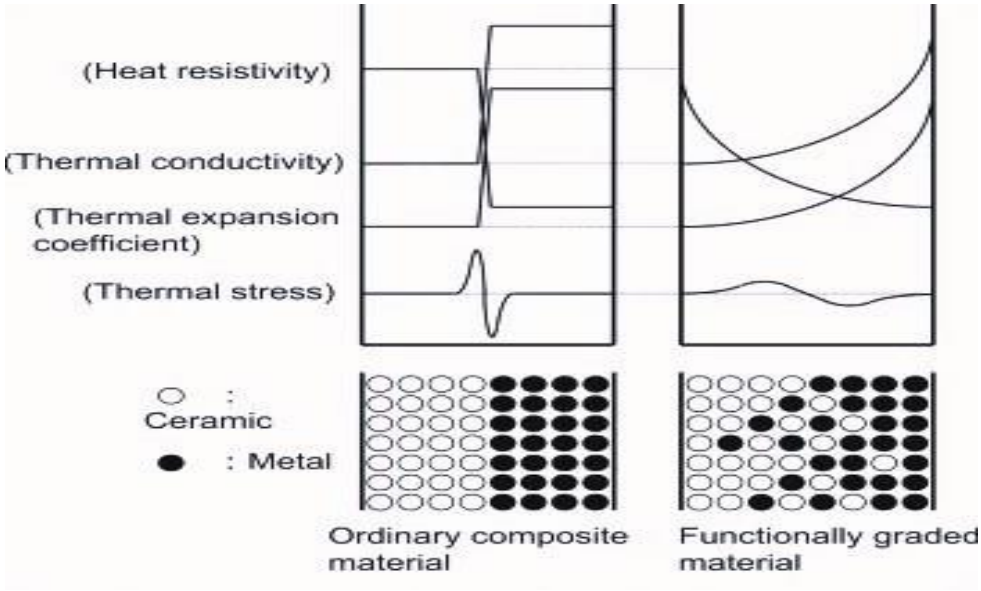

Figure I. 6 : material structures and properties of ordinary composite and functionally graded material

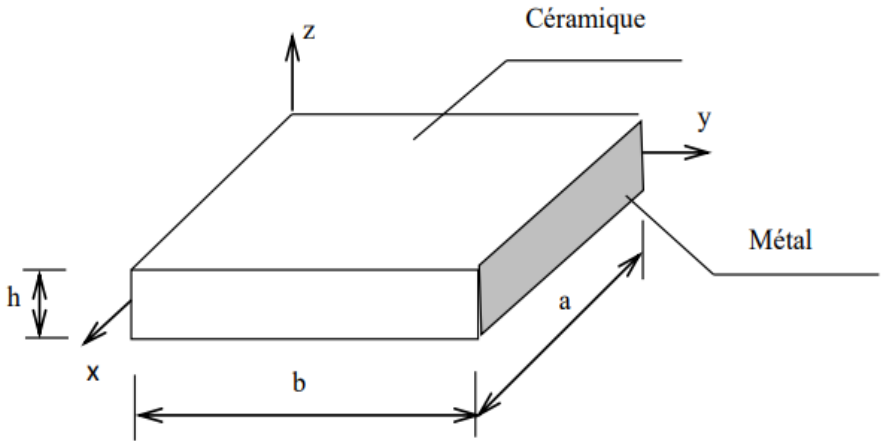

Figure I. 7 : Geometry of a FGM plate

The x and y coordinates define the plane of the rod, while the z-axis originates at the surface of the center of the row and in the thickness direction (fig. I. 7). The properties of the material including the Young module and the Fish coefficient on the upper and lower sides are different. They vary continuously, depending on the thickness (axis z), i.e.: E $= E(z)$ and $v = (z)$.

According to the study of (Jin, 1996), the fish coefficient on deformations is negligible compared to that of the Young module. Therefore, the Fish coefficient can be assumed as constant. However, the Young module in the direction of the thickness of the FGM beam varied according to the law of power (P–FGM), the exponential function (E-FGM) or with the sigmoid function (S- FGM).

I.5.1 Material properties of the P-FGM plate :

The volume fraction in P-FGMs is ensured by a law of power in the form:

$$V(z) = \left(\frac{1}{2} + \frac{z}{h}\right)^p \qquad \text{(I. 1)}$$

Where p is a parameter of the material and h is the thickness of the plate. Once the local volume fraction V(z) is defined, the material properties of a P-FGM plate can be determined by the law of mixtures:

$$E(z)=E_m + (E_C - E_m)V(z) \qquad \text{(I. 2)}$$

Where Em and $E_c$are Young's modules of the lower surface (z= $-\frac{h}{2}$) and the upper surface (z= $+\frac{h}{2}$) of the FGM plate, respectively.

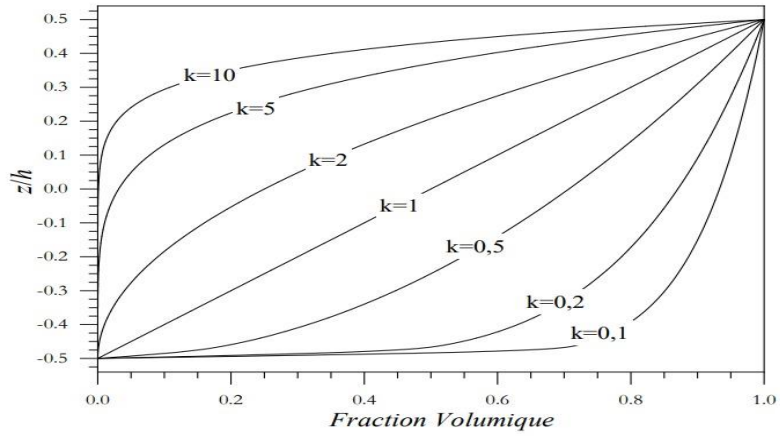

Figure I. 7 : The variation of the Young module through the thickness of a P-FGM plate

I.5.2 Material properties of S-FGM plate :

This model is determined using two functions of law of power (P-FGM).

This law enhances the distribution of constraints at each interface. This model is used to construct composite structures with several floors)Chi(2003 ،, and this law is provided by:

$$V_1(z) = \frac{1}{2}\left(\frac{z+h/2}{h/2}\right)^p, -h/2 \le z \le 0 \qquad \text{(I. 3)}$$

$$V_2 = 1 - \frac{1}{2}\left(\frac{z+h/2}{h/2}\right)^p, 0 \le z\, h/2 \qquad \text{(I. 4)}$$

The Young module of the S-FGM plaque may be calculated using:

$$E(z) = V_1(z)E_c + [1 - V_1(z)]E_m \quad \text{for} \quad -h/2 \le z \le 0 \qquad \text{(I. 5)}$$

$$E(z) = V_2(z)E_c + [1 - V_2(z)]E_m \quad \text{for} \quad 0 \le z \le h/2 \qquad \text{(I. 6)}$$

The (Fig. I. 9) Shows that the variation of the volume fraction defined by the equations (I.5) and (I.6) Represents the sigmoid distributions, and this FGM strap is called (S−FGM Power).

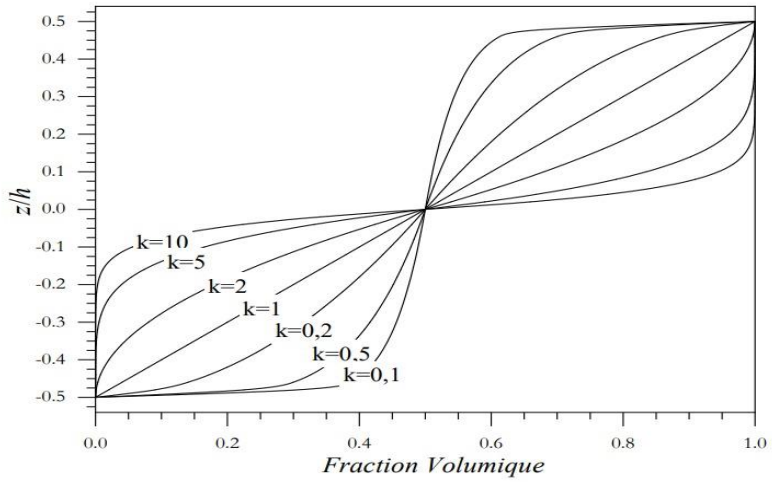

Figure I. 8 : The variation of the Young module through the thickness of a S-FGM plate

I.5.3 Material properties of the E-FGM plate :

Most researchers employ the exponential function, which is expressed in the form of, to characterize the material properties of GMF materials (Delale, 1983)

$$E(z) = E_2\, e^{B\left(z+\frac{h}{2}\right)} \qquad \text{(I. 7)}$$

With:

$$B = \frac{1}{h} ln\left(\frac{E_1}{E_2}\right) \qquad \text{(I. 8)}$$

The variation of the Young module through the thickness of the E-FGM beam is represented in (Fig I. 10).

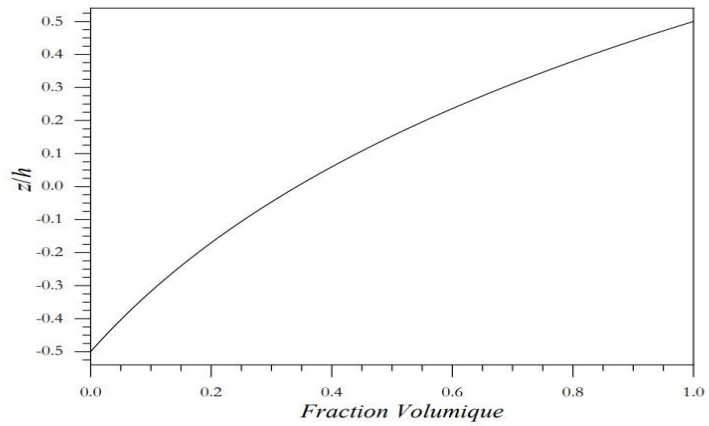

Figure I. 9 : The variation of the Young module through the thickness of an E-FGM plate

I.6 Conclusion

In this chapter, we endeavored to present a general overview of composite materials and functionally graded materials (FGM), firstly, we presented the fundamental notions as discussed, their development history, characteristics, and applications in the field of civil engineering, and outlining some advantages and some disadvantages that they can present. Finally, we ended by mentioning the different possible laws used to describe the variation of the material properties of FGM according to the plate thickness.

Chapter II. Theories of plates

II.1 Introduction

The structure of functionally graded materials can be considered as a heterogeneous body. Plate structures are one of the main load-bearing elements in various fields ofengineering such as civil, military, and automotive construction (Kolvik).

Such plates are often subjected to large in-plane compressive forces and/or shear loading. Different plate theories are available to describe the static and dynamic behavior of these plates. Depending on the plate geometry and material properties, it is of interest to utilize one plate theory over another. Understanding the differences between the theories, and the application of them, is of interest both to engineers working in the field of plate structures, aswell as researchers working with the development of new knowledge on plates.

Since the middle of the 19th century there has been ongoing research and development of plate theories. This research has resulted in three main categories in the field of plate theories:

- In1850: Kirchhoff plate theory, classical plate theory (CPT). Suitable for thin plates withthickness to width ratio less than 1/10. Ne -glects shear effects.

- In1950: Mindlin plate theory, first order shear deformation plate theory (FSDT). Suitablefor thick plates with thickness to width ratio more than 1/10. Includes shear effects.

- In1980: Higher order shear deformation plate theories (HSDT). Can represent the kinematicsbetter than FSDT and are especially suitable for composite plates. Includes shear effects (Kolvik).

High order theories were developed in response to the limitations of classical and first ordertheories, which were only applicable to thin and semi-thick plates. These theories helped to improve the assessment of the field of displacement variation via thickness plates (BENBAKHTI A, 2017).

II.2 Definition of plates

A plate is a defined solid. It is made up of two-dimensional, straight, flat structural elements whose lateral dimensions are large (a, b) and determined by a planar reference surface (x, y). These elements have a dimension known as thickness h. The thickness is typically measured on the plate's median surface and is typically constant, however it occasionally varies. We clarify (Figure II.1).

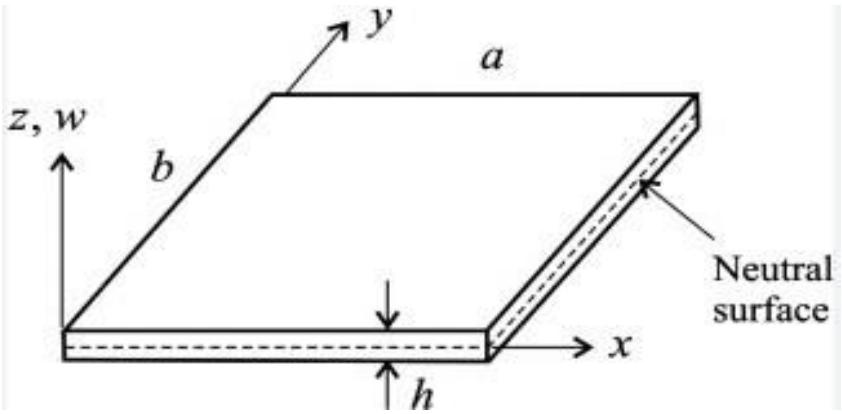

Figure II. 1 : Example of plate

II.3 Theories of single-layer plates (ESL):

II.3.1 Classical plate theory (CPT):

We start with the simplest and most general model, called the Love Kirchhoff model. This model is based on a linear distribution of displacements according to thickness. (E. Reissner, 1961).

It is commonly recognized that the elementary theory of beam flexion, upon which Euler-Bernoulli's theory is founded, ignores the effects of shear deformation. Furthermore, it is recognized that it is limited to thin beams (BOUAMAMA, 2019). The following presumptions underlie the Kirchhoff-Love hypothesis: A straight line that is perpendicular to the median plane exists before to deformation, and it stays straight, non-extensible, and normal to the mid-surface following deformation.

This theory is less true for thick beams when shear deformation is considerable since it assumes that transverse shear strains are low. Its application is restricted to thin plates and beams because of this assumption because they do not undergo large shear deformations. More sophisticated models that take shear deformation into account, like the Timoshenko beam theory, are needed to produce accurate findings for thicker structures. The Kirchhoff-Love

theory is also limited in its application in some cases since it ignores the effects of transverse normal stress. Notwithstanding these drawbacks, the Kirchhoff-Love hypothesis is frequently applied in engineering applications involving thin beams and plates because of its ease of use and efficacy.

These three assumptions lead to transverse distortions being omitted, $(\varepsilon_{zz})$and (ε_{yz}). Because the product of $(\varepsilon_{zz})$and (σ_{zz}) equals zero in the plate's total potential energy, ignoring (ε_{zz})leads to omitting(σ_{zz}) (Ochoa, 1992).

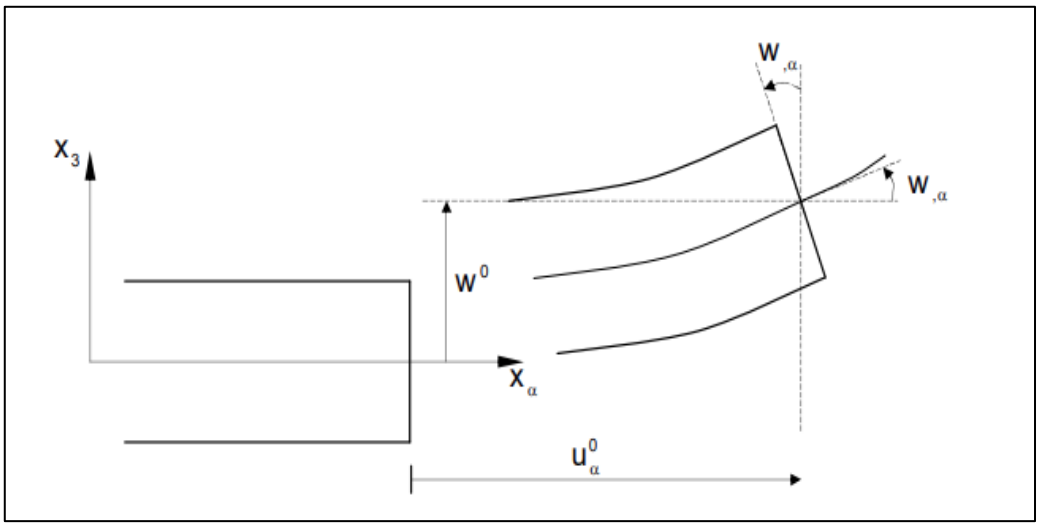

Figure II. 2 : Love-Kirchhoff Cinematic.

The Love-Kirchhoff movement field is then written,

$$U(x, y, z) = U_0(x, y, z,) - z\frac{\delta W_0}{\delta_x}$$

$$V(x, y, z) = V_0(x, y, z,) - z\frac{\delta W_0}{\delta_Y}$$

$$W(x, y, z) = W_0(x, y, z) \qquad \text{(II. 1)}$$

With, U_0, V_0, W_0 are the components of the displacement field on the middle plane of the plate (z=0).

II.3.2 First order shear deformation theory (FSDT):

Deformations resulting from transverse shear must be considered in plates with a reasonablethickness. The first order deformation theory incorporates the transverse shear effect while drawing on classical theory. Nonetheless, since the deformations are continuous

throughout the plate's thickness, a shear correction factor must be added. The authors of this first order shear strain theory (FSDT) are Mindlin (1950) and Reissner (1945).

Its foundation is the Mindlin kinematic hypothesis, which states that due of transverse shear, the normal in the deformed configuration stays straight but is not perpendicular to the average surface (Figure II. 3) (Guellil M. S.-Z., 2021).

The first-order theory is based on the following field of motion:

$$\begin{aligned} U(x,y,z) &= U_0(x,y) + Z\,\emptyset_X\ (x,y) \\ V(x,y,z) &= V_0(x,y) + Z\,\emptyset_Y\ (x,y) \\ W(x,y,z) &= W_0(x,y) \end{aligned} \qquad \text{(II. 2)}$$

With: (U_0, V_0, W_0) and ($\emptyset_X$, $\emptyset_Y$) are the membrane displacements and rotations around the x and y axes, respectively.

In view of that displacement field the strains are given by:

$$\begin{aligned} \varepsilon_x &= \frac{\partial_u}{\partial_x} = z\frac{\partial_{\emptyset x}}{\partial_x} \\ \varepsilon_y &= \frac{\partial_v}{\partial_y} = z\frac{\partial_{\emptyset y}}{\partial_y} \\ \gamma_{xy} &= \frac{\partial_u}{\partial_y} + \frac{\partial_v}{\partial_x} = z\left(\frac{\partial_{\emptyset x}}{\partial_y} + \frac{\partial_{\emptyset y}}{\partial_x}\right) \\ \gamma_{xz} &= \frac{\partial_u}{\partial_z} + \frac{\partial_w}{\partial_x} = \emptyset x + \frac{\partial_w}{\partial_x} \\ \gamma_{yz} &= \frac{\partial_v}{\partial_z} + \frac{\partial_w}{\partial_y} = \emptyset y + \frac{\partial_w}{\partial_y} \end{aligned} \qquad \text{(II. 3)}$$

Assuming the plate material is isotropic and obeys Hooke's law the stress strain relationship is given by:

$$\begin{aligned} \sigma_x &= \frac{E}{1-v^2}\left(\epsilon_x + v\epsilon_y\right) \\ \sigma_y &= \frac{E}{1-v^2}\left(\epsilon_y + v\epsilon_x\right) \\ \sigma_{xy} &= G\,\gamma_{xy} = \frac{E}{2(1+v)}\gamma_{xy} \\ \sigma_{xz} &= G\,\gamma_{xz} = \frac{E}{2(1+v)}\gamma_{xz} \\ \sigma_{yz} &= G\,\gamma_{yz} = \frac{E}{2(1+v)}\gamma_{yz} \end{aligned} \qquad \text{(II. 4)}$$

The displacement field defined in the above expression enables the continuation of the classical plaque theory described in the last part by replacement.

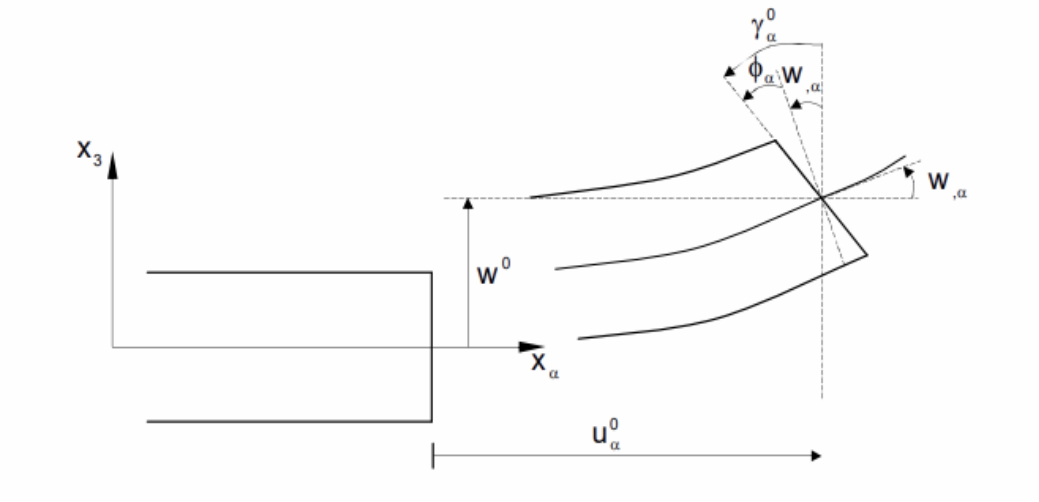

Figure II. 3: Schematization of plate deformations using the "FSDT" theory.

Furthermore, high order shear deformation theories have been established in order to preventthe inclusion of a correction factor.

In fact, $f(z) = 0$ is used to acquire the displacements in classical plate theory (CLPT), whereas $f(z) = z$ is used to produce first-order theory (FSDT).

The (Figure II. 4) shows the variation of the function shape as well as its derivation relative to the thickness of the plate. This variation is more authentic for the case of layered plates or at the level of the interface there is a discontinuity of the distribution of properties while for FGMs this problem is solved.

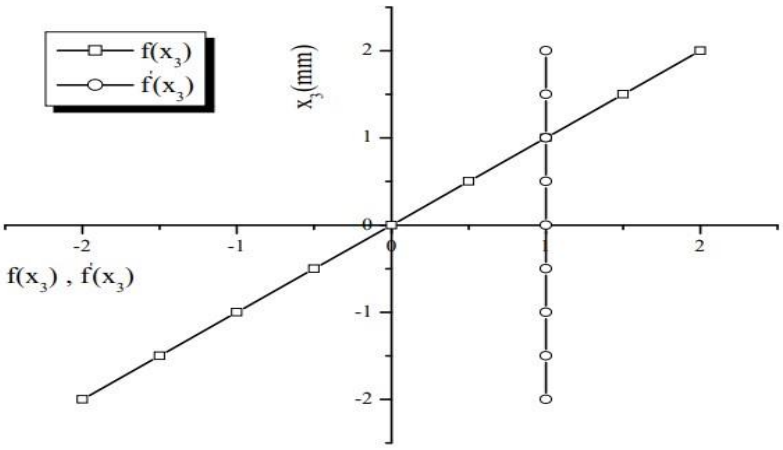

Figure II. 4 : Variation of the left function according to thickness.

II.3.3 Higher shear deformation theory (HSDT):

Unlike the CPT and FSDT theories, which assume a linear distribution of displacement across thickness, the high order theory is based on a nonlinear distribution of fields in thickness. As such, the effects of transverse normal strain and/or transverse shear strain are taken into account. (Hildebrand, 1949), (Naghdi, 1957), (Reissner, 1975), (Reddy, 1984), and (Kant, 2002)are a few sources that discuss these models.

We have introduced four plate models to study the behavior of materials with gradient characteristics (BOUKHARI, 2016). These models provide a more realistic depiction of the distribution of stress and strain by accounting for differences in material properties caused by plate thickness. Gradient characteristics are crucial to understanding the mechanical behavior of functionally graded materials (FGMs), whose composition and structure change continuously. These sophisticated plate theories allow for a more accurate prediction of FGM performance under different loading scenarios. This method is very useful for creating parts for high-performance engineering applications including automotive, aerospace, and others where FGMs are being used more and more.

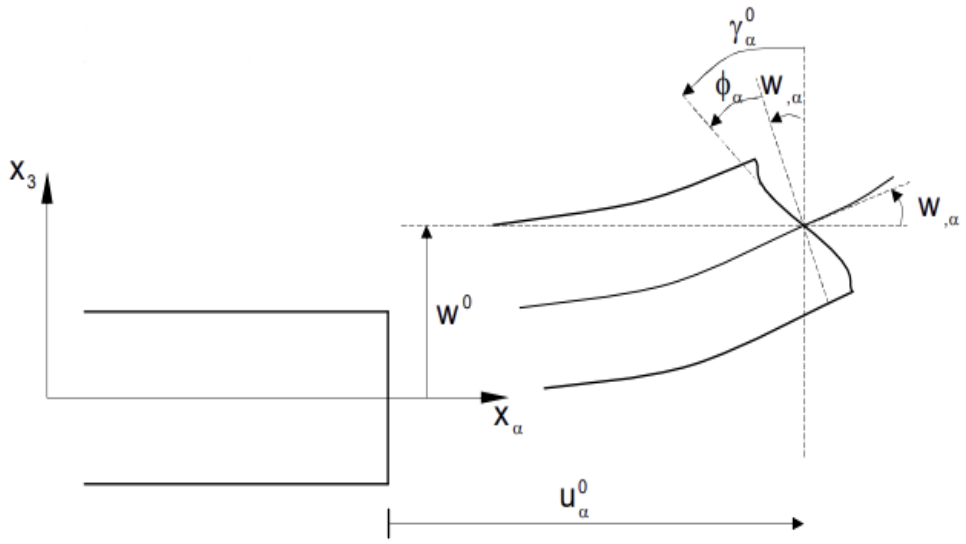

Figure II. 5 : Schematization of plate deformations using the “HSDT” theory.

The displacement field for a plate in HSDT can be described by:

$$\mathrm{U}(\mathrm{x},\mathrm{y},\mathrm{z}) = U_0(\mathrm{x},\mathrm{y}) - zw_x + \mathrm{f}(z)(\emptyset_{\mathrm{X}} + w_x)$$

$$\mathrm{V}(\mathrm{x},\mathrm{y},\mathrm{z}) = V_0(\mathrm{x},\mathrm{y}) - zw_y + \mathrm{f}(z)(\emptyset_{\mathrm{y}} + w_y)$$

$$W(x,y,z) = W_0(x,y) \qquad \text{(II. 5)}$$

The in-plane displacement of the middle surface (u0 and v0) will in the following be omitted without affecting the basic bending features of shear flexible plates.

In view of that displacement field the strains are given by:

$$\varepsilon_x = \frac{\partial_u}{\partial_x} = -zw_{xx} + f(z)(\emptyset_{xx} + w_{xx}) = f(z)\emptyset_{xx} + [f(z) - z]w_{xx}$$

$$\varepsilon_y = \frac{\partial_u}{\partial_y} = -zw_{yy} + f(z)(\emptyset_{yy} + w_{yy}) = f(z)\emptyset_{yy} + [f(z) - z]w_{yy}$$

$$\gamma_{xz} = \frac{\partial_u}{\partial_z} + \frac{\partial_w}{\partial_x} = f'(z)(\emptyset_x + w_x)$$

$$\gamma_{yz} = \frac{\partial_v}{\partial_z} + \frac{\partial_w}{\partial_y} = f'(z)(\emptyset_y + w_y)$$

$$\gamma_{xy} = \frac{\partial_u}{\partial_y} + \frac{\partial_v}{\partial_x}$$

$$= -zw_{xy} + f(z)(\emptyset_{xy} + w_{xy}) - zw_{yx} + f(z)(\emptyset_{yx} + w_{yx})$$

$$= f(z)\emptyset_{xy} + [f(z) - z]w_{xy} + f(z)\emptyset_{yx} + [f(z) - z]w_{yx} \qquad \text{(II. 6)}$$

Organizing the above strain expressions to release the gradients of the deflection (w) and rotations ($\emptyset_{\mathrm{X}}$)and ($\emptyset_{\mathrm{y}}$):

$$\varepsilon_x = z\emptyset_{xx} + (f(z) - z)(w_{xx} + \emptyset_{xx})$$

$$\varepsilon_y = z\emptyset_{yy} + (f(z) - z)(w_{yy} + \emptyset_{yy})$$

$$\gamma_{xz} = f'(z)[w_x + \emptyset_x]$$

$$\gamma_{yz} = f'(z)[w_y + \emptyset_y]$$

$$\gamma_{xy} = z\emptyset_{xy} + (f(z) - z)(w_{xy} + \emptyset_{xy}) + z\emptyset_{yx} + (f(z) - z)(w_{yx} + \emptyset_{yx}) \qquad \text{(II. 7)}$$

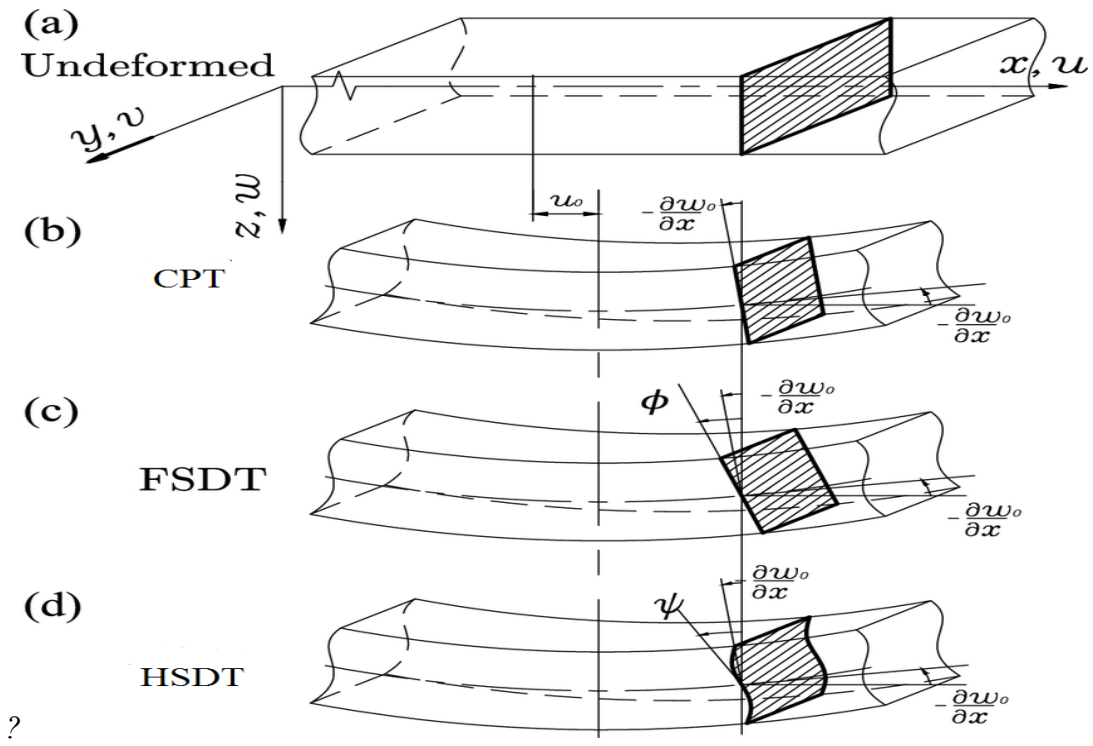

Figure II. 6 : Description of the deformation of a plate according to theories: classical (CLPT), first order (FSDT) and high order (HSDT).

The following conditions must be met in order for the tangential constraints to be zero on the beam's extreme edges:

$$f'(z)\ \big|_{z=\pm\frac{h}{2}} = 0 \qquad \text{(II. 8)}$$

This is the condition that allows us to have a parabolic distribution of cutting stresses on the thickness of the bar on the one hand and to correctly choose the functions that meet the condition (II. 8).

These are a few significant additions to the advancement of higher-order models that stand out in the literature and have different forms' functions $f(z)$.

II.3.4 Review of the different models of high order theory :

Ambartsumyan's approach (Ambartsumyan, 1969)with;

$$f(z) = \frac{z}{2}\left(\frac{h^2}{4} - \frac{z^2}{3}\right) \qquad \text{(II. 9)}$$

The Reissner approach (Reissner, 1945) with;

$$f(z) = \frac{5}{4} z \left(1 - \frac{4z^2}{3h^2}\right) \quad \text{(II. 10)}$$

Levinson, Murthy and Reddy's Approach (Murthy, 1981) (Reddy J.N, 1999) With;

$$f(z) = z \left(1 - \frac{4z^2}{3h^2}\right) \quad \text{(II. 11)}$$

The Touratier's Approach (Touratier, 1991)with;

$$f(z) = \frac{h}{\pi} sin \left(\frac{z}{h}\right) \quad \text{(II. 12)}$$

Touratier's "sinus" model (SSDT), in contrast to earlier higher-order models, is not dependent on a polynomial function. Thus, a sinusoidal trigonometric function is introduced to represent the distribution of shear stresses through the thickness. A more realistic depiction of the shear stress variation within the beam is possible with this approach. As a result, the transverse shear stresses as defined by the sinusoidal patterns assume a sinusoidal shape, offering a more accurate representation of the distribution of stresses. This approach improves the model's accuracy, particularly for thick beams where shear deformation is substantial.(Belkacem, 2015).

Recently, Afaq and all proposed an exponential model with advanced kinematics.
The transverse cutting function is of the following shape:

$$f(z) = ze^{-2\left(\frac{z}{h}\right)^2} \quad \text{(II. 13)}$$

The Touratier "sinus" function allows development in uneparable powers, but the exponential function option provides development in equal and unmatched powers of the variable z (ABDELBARI, 2016).

The Aydogdu approach (Aydogdu, 2005)with;

$$f(z) = z\alpha^{\frac{-2\left(\frac{z}{h}\right)^2}{ln(\alpha)}} \qquad \alpha > 0 \quad \text{(II. 14)}$$

h: being the thickness of the FGM plate.

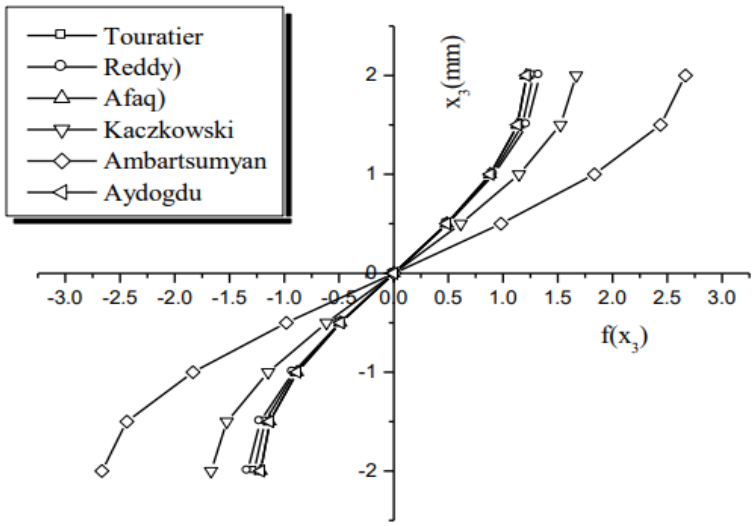

Figure II. 7 : Variation of the f(z) shape function of the different models depending on the thickness.

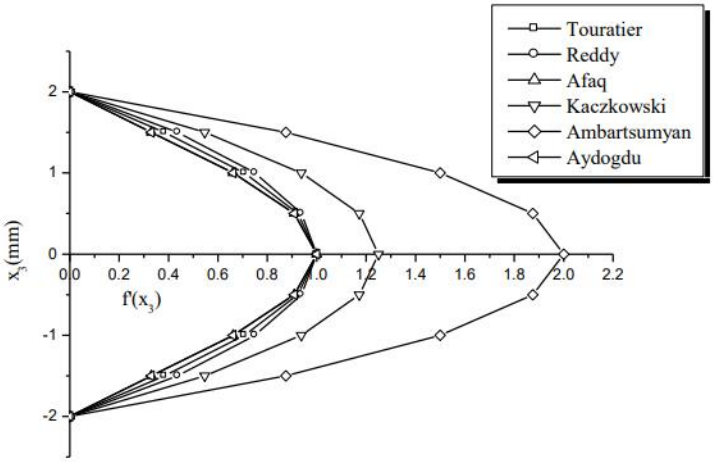

Figure II. 8 : Variation of the derivative of the shape function f '(z) of different patterns according to thickness.

II.4 Conclusion

The theory of plates and the analytical models of FGM plates the higher shear deformation theory (HSDT), the first-order shear deformation theory (FSDT), and the classical plate theory (CPT) have all been briefly examined in this chapter. The kinematic equations of each point in the plate based on the generalized displacement are formulated using the hypotheses of each theory in a two-dimensional approach to elasticity. It should be noted that different ideas that are formed from the theories discussed in this chapter occasionally produce findings that are acceptable. So, the ideas that are most frequently employed in literature piqued our curiosity.

We also find that, in contrast to traditional composites, there is no sharp shift in mechanical properties with FGM materials, and lamination is an inescapable issue, making the corresponding one-layer technique more appropriate for these materials.

Additionally, it seems that high-order theories are attractive from a precise standpoint, but they are still a challenge in terms of formulation and difficult to calculate.

ChapterIII. Analysis of free vibrations of FG plates with porosity variations using FSDT

III.1 Introduction

The Functionally graded materials (FGMs) offer tailored mechanical properties, making them attractive for structural applications. Grading along the thickness direction allows for optimized performance under various loading conditions. This study aims to analyze the influence of grading patterns and porosity disruptions on the mechanical behavior of FGM plates.

To determine how three grading patterns P-FGM, E-FGM, and S-FGM affect material qualities, they are studied. The distributions for P-FGM, E-FGM, and S-FGM are power-law, exponential, and sigmoid, respectively. Every pattern has unique benefits and difficulties that have an impact on how FGM plates respond mechanically.

To examine their impacts on FGM plates, four types of porosity disruptions Type A, Type B, Type C, and Type D are introduced. These interruptions could be brought on by faults in the material processing or the manufacturing process. It is essential to understand their impact on mechanical properties when creating durable constructions.

III.2 FGM performance with porosity :

This work looks at materials with a gradient of porous functionality (FGM) in structural plates that are gradated along the axis z in the direction of thickness. The center plan serves as a reference for the cartesian coordinate system, and the material composition varies from metal enrichment at the bottom to ceramic enrichment at the top. The three geometric characteristics are thickness (h), length (a), and size (b). To shed light on the evolution of material properties, the power law gradation (P-FGM), exponential (E-FGM), and sigmoid (S-FGM) schemes are studied. Furthermore, as shown in Figure 1, four different forms of porosity perturbations types A, B, C, and D are taken into consideration.

The theory of deformation by first-order shear (FSDT) is used to model the mechanical behavior of these functionally graded materials (FGM), providing a more accurate representation than the conventional theory of plates by including the effects of shear deformation. The properties of the materials are assumed to continuously vary with thickness in accordance with the selected gradation scheme, influencing the distribution of constraints and overall structural performance. Digital simulations are used to analyze the static and dynamic responses of FGM plaques under various charging settings. The results clearly show how porosity perturbations affect mechanical behavior and provide information for optimizing FGM concepts to enhance performance and durability (Hu, 2023).

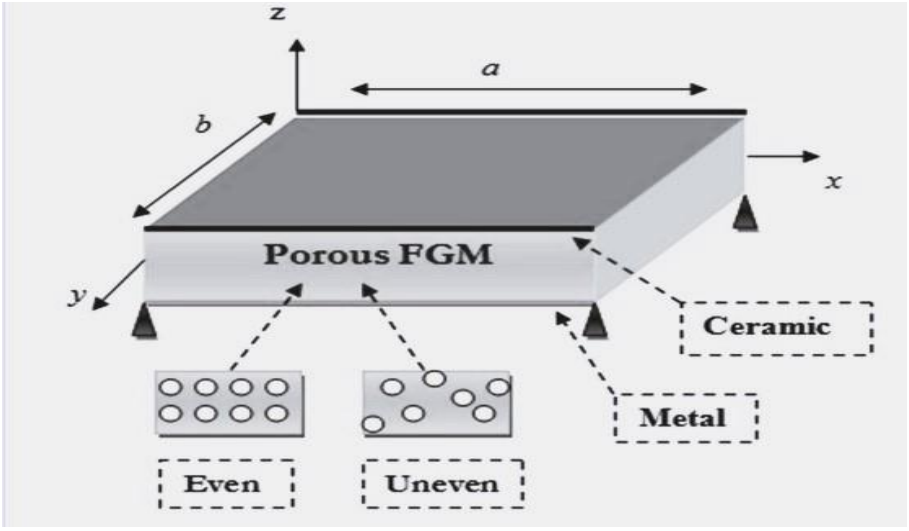

Figure III. 1: Geometric models of porous FGM plates with different structures.

When the elastic modulus varies in a given direction, it can be described as follows using the power-law function:

$$P = P_m + (P_c - P_m)(1/2 + z/h)^p - \frac{\lambda_0}{2}(P_c + P_m)\,V_j \qquad (\text{III}.1)$$

The elastic modulus fluctuation in a given direction can be represented using the exponential function as follows:

$$P = P_c e^{(\ln(\frac{P_m}{P_c})(1-\left(\frac{1}{2}+\frac{z}{h}\right)^p)} - \frac{\lambda_0}{2}(P_c + P_m)V_j \qquad (\text{III}.2)$$

It is also possible to specify the material properties of porous FGM plates using a sigmoid function.

For $0 \le z \le {}^{h}/_{2}$

$$P = P_m + (P_c - P_m)[1 - \frac{1}{2}(1 - \frac{2z}{h})^p] - \frac{\lambda_0}{2}(P_c + P_m)\,V_j \qquad (\text{III}.3)$$

For $-{}^{h}/_{2} \le z \le 0$

$$P = P_m + (P_c - P_m)[\frac{1}{2}(1 + \frac{2z}{h})^p] - \frac{\lambda_0}{2}(P_c + P_m)\,V_j \qquad (\text{III}.4)$$

The gradient variation of the material in the direction of thickness is denoted by P, which stands for the physical parameters (Young's modulus, density, and Poisson's ratio). Metal and ceramic are denoted by the subscripts m and c, respectively. V_j(j=A, B, C, D) indicates the four porosity distributions, z specifies any position in the thickness direction, p indicates gradient index, and $\lambda_0$indicates porosity. The volume percentages of metal and ceramic in the plates are related to one another.

$$V_c + V_m = 1 \qquad (\text{III}.5)$$

The different porosity distributions V_j are adjusted further as

$$V_A = 1 \qquad (\text{III}.6)$$

$$V_B = 1 - \frac{2|z|}{h} \qquad (\text{III}.7)$$

$$V_c = \frac{2|z|}{h} \qquad (\text{III}.8)$$

$$V_D = \frac{1}{2} - \frac{z}{h} \qquad (\text{III}.9)$$

Where subscript A represents a symmetrical and even distribution, while subscripts B, C, and D stand for other uneven symmetrical distributions.

The Young's modulus distribution over the dimensionless thickness of plates for three grading patterns with various porosity distributions. The default material combination is AlAl_2O_3.The porosity λ_0=0.3 and gradient index p=2 is set here to show the difference where gradient index p=1, and the P-FGM and S-FGM functions are identical.

III.3 The constituent relationships :

FSDT is used in this task to offer the kinematic assumption for the displacement of theFGM plate, and the equation for the displacement field is determined (Hu, 2023):

$$U(x, y, z, t) = u(x, y, t) + z\emptyset_x(x, y, t)$$

$$V(x, y, z, t) = v(x, y, t) + z\emptyset_y(x, y, t) \qquad (\text{III}.10)$$

$$W(x, y, z, t) = w(x, y, t)$$

Where U, V and W are the displacement along les directions x, y and z, and u, v, w arethe displacement on the neutral surface. Øx and Øy and t is time denote the rotations of theplans xz and yz due to flexion, respectively (Nguyen, 2019).

As the FSDT does not include the calculation of stress-strain in the Z-direction, the displacement field is connected to the linear strain-displacement relationship by (Hu,2023):

$$\begin{Bmatrix} \varepsilon_x \\ \varepsilon_y \\ \gamma_{xy} \end{Bmatrix} = \begin{Bmatrix} \frac{\partial_u}{\partial_x} + z\frac{\partial \emptyset_x}{\partial_x} \\ \frac{\partial_v}{\partial_y} + z\frac{\partial \emptyset_y}{\partial_y} \\ \frac{\partial_u}{\partial_y} + \frac{\partial_V}{\partial_x} + z\frac{\partial \emptyset_x}{\partial_y} + z\frac{\partial \emptyset_y}{\partial_x} \end{Bmatrix}$$

$$\begin{Bmatrix} \gamma_{xz} \\ \gamma_{yz} \end{Bmatrix} = \begin{Bmatrix} \emptyset_x + \frac{\partial_w}{\partial_x} \\ \emptyset_y + \frac{\partial_w}{\partial_y} \end{Bmatrix} \qquad (\text{III}.11)$$

To address the discrepancy between theoretical and actual stress, the approach involves incorporating shear correction factors (SCF) and applying linear constitutive relationshipsto the porous FGM plate.

$$\begin{Bmatrix} \sigma_x \\ \sigma_y \\ \tau_{xy} \end{Bmatrix} = \begin{bmatrix} Q_{11} & Q_{12} & 0 \\ Q_{12} & Q_{22} & 0 \\ 0 & 0 & Q_{66} \end{bmatrix} \begin{Bmatrix} \varepsilon_x \\ \varepsilon_y \\ \gamma_{xy} \end{Bmatrix} \text{ and } \begin{Bmatrix} \tau_{yz} \\ \tau_{xz} \end{Bmatrix} = \begin{bmatrix} Q_{44} & 0 \\ 0 & Q_{55} \end{bmatrix} \begin{Bmatrix} \gamma_{yz} \\ \gamma_{xz} \end{Bmatrix} \qquad (\text{III}.12)$$

Where $(\sigma_x, \sigma_y, \tau_{xy}, \tau_{yz}, \tau_{xz})and(\varepsilon_x, \varepsilon_y, \gamma_{xy}, \gamma_{yz}, \gamma_{xz})$ are the deformation and contra intrusion components, respectively.

Using the material properties specified in the equation, the coefficients of rigidity can be expressed as follows:

$$Q_{11} = Q_{22} = \frac{E(z)}{1-\mu(z)^2} \qquad Q_{12} = \frac{\mu(z)E(z)}{1-\mu(z)^2}$$

$$Q_{44} = Q_{55} = Q_{66} = \frac{E(z)}{2(1+\mu(z))} \qquad (\text{III}.13)$$

The equation of motion can be quantified using the Hamilton's principle that is:

$$\int_{t_1}^{t_2}(\delta U - \delta K)dt = 0 \qquad (\text{III}.14)$$

Where δU is the variation of stain energy, δV is the variation of work done by externalforces, andδK is the variation of kinetic energy. The expression of δU is:

$$\delta U = \int_v \int_{-\frac{h}{2}}^{\frac{h}{2}} (\sigma_x \delta\, \varepsilon_x + \sigma_y \delta\varepsilon_y + \tau_{xy}\delta\gamma_{xy} + \tau_{xz}\delta\gamma_{xz} + \tau_{yz}\delta\gamma_{yz})dzdA \qquad (\text{III}.15)$$

Where N, M, and Q are the stress resultants, which are defined by:

$$\left\{ \begin{pmatrix} N_x \\ N_y \\ N_z \end{pmatrix}, \begin{pmatrix} M_x \\ M_y \\ M_z \end{pmatrix} \right\} = \int_{-h/2}^{h/2} \begin{pmatrix} \sigma_x \\ \sigma_y \\ \tau_{xy} \end{pmatrix} (1, z)\, dz \qquad (\text{III}.16)$$

$$\begin{pmatrix} Q_{xz} \\ Q_{yz} \end{pmatrix} = \int_{-h/2}^{h/2} \begin{pmatrix} \tau_{xz} \\ \tau_{yz} \end{pmatrix} dz \qquad (\text{III}.17)$$

The expression of variation of kinetic energy δK is:

$$\delta K = \int_{t_1}^{t_2} (\dot{u}\,\delta\dot{u} + \dot{v}\delta\dot{v} + \dot{w}\delta\dot{w})\rho(z)\,dV \qquad (\text{III}.18)$$

After integrating equation (III.18) over the thickness direction, equation (III.18) becomes:

$$\delta K = \int_{t_1}^{t_2} \{I_0[\dot{u}\delta\dot{u} + \dot{v}\delta\dot{v}]\} \qquad (\text{III}.19)$$

Where:

$$\begin{pmatrix} I_0 \\ I_1 \\ I_2 \end{pmatrix} = \int_{-h/2}^{h/2} \rho(z) \begin{pmatrix} 1 \\ z \\ z^2 \end{pmatrix} dz \qquad (\text{III}.20)$$

Substituting equation (III.15), (III. 19) into equation (III.14) and integrating par parts, the equations of motions are obtained as :

$$\delta u = \frac{\partial N_x}{\partial_x} + \frac{\partial N_{xy}}{\partial_y} = I_0 \frac{\partial^2 u}{dt^2} + I_1 \frac{\partial^2 \emptyset_x}{dt^2} \qquad (\text{III}.21)$$

$$\delta v = \frac{\partial N_y}{\partial_y} + \frac{\partial N_{xy}}{\partial_x} = I_0 \frac{\partial^2 v}{dt^2} + I_1 \frac{\partial^2 \emptyset_x}{dt^2} \qquad (\text{III}.22)$$

$$\delta w = \frac{\partial \emptyset_{xz}}{\partial_x} + \frac{\partial \emptyset_{yz}}{\partial_z} = I_0 \frac{\partial^2 w}{dt^2} \qquad (\text{III}.23)$$

$$\delta \emptyset_x = \frac{\partial M_x}{\partial_x} + \frac{\partial M_{xy}}{\partial_y} = I_1 \frac{\partial^2 u}{dt^2} + I_2 \frac{\partial^2 \emptyset_x}{dt^2} \qquad (\text{III}.24)$$

$$\delta \emptyset_y = \frac{\partial M_y}{\partial_y} + \frac{\partial M_{xy}}{\partial_x} = I_1 \frac{\partial^2 v}{dt^2} + I_2 \frac{\partial^2 \emptyset_x}{dt^2} \qquad (\text{III}.25)$$

III.4 Analytical solution :

Employing the Navier solution, the solutions of the plate were assumed as:

$$\begin{Bmatrix} u\,(x,y,t) \\ v\,(x,y,t) \\ w\,(x,y,t) \\ \emptyset_x\,(x,y,t) \\ \emptyset_y\,(x,y,t) \end{Bmatrix} = \sum_{m=1}^{M} \sum_{n}^{N} \begin{Bmatrix} U_{mn}\,(t)\ \cos\alpha x\ \sin\beta y \\ V_{mn}\,(t)\ \sin\alpha x\ \cos\beta y \\ W_{mn}\,(t)\ \sin\alpha x\ \sin\beta y \\ X_{mn}\,(t)\ \cos\alpha x\ \sin\beta y \\ Y_{mn}\,(t)\ \sin\alpha x\ \cos\beta y \end{Bmatrix} \qquad (\text{III}.26)$$

Where $\alpha = m\pi/b$, $\beta = m\pi/a$, (Umn, Vmn, Wmn, Xmn, Ymn) quantities to be determined m, n are mode numbers.

$$m= n =1 \qquad (\text{III}.27)$$

The free vibration equation is expressed in matrix form:

$$(\mathrm{K} - \omega^2\mathrm{M})\Delta= 0 \qquad (\text{III}.28)$$

Where K and M are, respectively, the stiffness matrix, Δ is the vector of unknown Coefficients , and ω is the frequency of free vibration. The elements of K, M and Δ are as Follows :

$$k = \begin{bmatrix} L_{11} & L_{12} & L_{13} & L_{14} & L_{15} \\ L_{21} & L_{22} & L_{23} & L_{24} & L_{25} \\ L_{31} & L_{32} & L_{33} & L_{34} & L_{35} \\ L_{41} & L_{42} & L_{43} & L_{44} & L_{45} \\ L_{51} & L_{52} & L_{53} & L_{54} & L_{55} \end{bmatrix}, \Delta= \begin{bmatrix} U_{mn} \\ V_{mn} \\ W_{mn} \\ X_{mn} \\ Y_{mn} \end{bmatrix}, M = \begin{bmatrix} I_0 & 0 & 0 & I_1 & 0 \\ 0 & I_0 & 0 & 0 & I_1 \\ 0 & 0 & I_0 & 0 & 0 \\ I_1 & 0 & 0 & I_2 & 0 \\ 0 & I_1 & 0 & 0 & I_2 \end{bmatrix} \qquad (\text{III}.29)$$

$L_{ij} = L_{ji}$

$L_{11} =\propto^2 A_{11} + \beta^2 A_{66}$, $\quad L_{12} = L_{21} =\propto \beta(A_{12} + A_{66})$

$L_{14} = L_{41} =\propto^2 B_{11} + \beta^2 B_{66}$, $\quad L_{15} = L_{51} =\propto \beta(B_{12} + B_{66})$

$\mathrm{L}_{22} =\propto^2 \mathrm{A}_{66} + \beta^2 \mathrm{A}_{22}$, $\quad \mathrm{L}_{24} = \mathrm{L}_{42} =\propto \beta(\mathrm{B}_{21} + \mathrm{B}_{66})$

$L_{33} =\propto^2 A_{55} + \beta^2 A_{44}$, $\quad L_{34} = L_{43} =\propto A_{55}$ $\qquad (\text{III}.30)$

$L_{44} =\propto^2 D_{11} + \beta^2 D_{66} + A_{55}$, $\quad L_{13} = L_{31} = L_{23} = L_{32} = 0$

$L_{45} = L_{54} =\propto \beta(D_{12} + D_{66})$, $\quad L_{53} = L_{35} = \beta A_{44}$

$L_{55} =\propto^2 D_{66} + \beta^2 D_{22} A_{44}$

III.5 Conclusion

This chapter examined the free vibration analysis of a functionally graded plate using FSDT while taking shear deformation into account. The FG plate's motion is governed by Hamilton's principle, which was the basis for solving the governing equations that were obtained using the Navier technique. To find out how different factors, like grading patterns and porosity disruptions, affect the plate's vibrational properties, numerical results were produced. The research offers a more profound comprehension of the dynamic behavior of materials with functional grades, which aids in the creation of stronger and more effective structures.

Chapter Ⅳ. Results and discussion

IV.1 Introduction

This section examines the effects of several geometric and material characteristics on the mechanical performance of functionally graded material (FGM) plates. After the calculating procedure outlined in the previous chapter is finished, this section will present detailed results using tables and graphs. In addition, three verification processes are performed to ensure the accuracy of the proposed theory. First, a comparison with studies that compute frequencies using analytical solutions is given, showing that different theoretical models agree with each other. Second, the ideal Al/Al2O3 plate's frequencies are computed using the proposed theory, and the results show good agreement with material parameters reported in the literature.
Finally, the effect of porosity on the frequency of the plate is examined through comparisons with the (Kumar, 2023) study. The methodology is validated as consistent results are discovered, even with modifications in the parameterK_s.

Furthermore, parametric experiments are carried out to assess how various grading patterns affect the mechanical performance of FGM plates. The findings are displayed in detail in tables and graphs that show how the stress distribution and deformation change with different loading scenarios. To provide a comprehensive understanding of the structural performance of FGM plates, the impacts of plate aspect ratios and boundary conditions on the vibrational properties are also examined. This thorough research helps to optimize the design of FGM for certain technical applications, guaranteeing improved performance and durability.

IV.2 Verification of analytical solution :

In this section, we determine the bending of FG plates using the recently developed theory. We keep Poisson's ratio constant at ν = 0.3 and contrast our findings with previously published solutions. We employ numerical case studies to verify the precision of our analysis. The aluminum and alumina that make up the FG plate have the following material characteristics:

- Metal (Aluminum, Al): Em = 67 GPa; ν = 0.3;$\rho_m = 2702 Kg/m^3$.
- Ceramic (Alumina, Al_2O_3): Ec = 349.55 GPa, ν = 0.3;$\rho_c = 3800 Kg/m^3$.

Table IV.1: Parameters of ceramic and metal materials made in FGM plates

Material	Al	Al_2O_3	SiC	Si_3N_4
Youngs modulus/GPa	67	349.55	302	348.45
Poisson's ratio	0.3	0.26	0.17	0.24
Density(kg/m^3)	2702	3800	3100	2370

The numerical results are presented in terms of non-dimensional frequencies. The non-dimensional natural frequency parameter is defined as:

$$\overline{w} = wh\sqrt{\frac{\rho_c}{E_c}} \qquad \text{(IV. 1)}$$

IV.3 Effect of porosity and gradient index :

IV.3.1 Example 1:

A comparative analysis with research using analytical solutions to determine frequencies is shown in Table Ⅳ.1.(R. Bennai, 2019) uses HSDT as its framework and compares non-dimensional frequency ($\overline{w} = wh\sqrt{\rho_c/E_c}$). Based on the suggested theory, frequencies of an ideal Al/Al_2O_3 plate with a consistent aspect ratio of a/b=1 and consistent material properties as reported in the literature are computed. Table Ⅳ.2 presents the non-dimensional frequencies determined by HSDT ,and FSDT in different modes, taking into account gradient indexes (p=0,0.5,1,4,10) and varying width-to-thickness ratios ($a/h = 5,10$). Table Ⅳ.3 illustrates the good agreement between the data from HSDT and the results of this paper. It has been observed that the frequency values obtained by both methods are relatively similar. The finite element simulation presents configuration difficulties, which can lead to errors, but the values remain within acceptable limits.

Table IV.2: Data comparison of non-dimensional frequency of FGM plates using analytical solution

a/h	Mode (m, n)	Theory	Gradient index p				
			P=0	P=0.5	P=1	P=4	P=10
5	(1,1)	(R. Bennai, 2019)	0.2122	0.1825	0.1659	0.1409	0.1318
		(Hosseini-Hashemi, 2011)	0.2113	0.1807	0.1631	0.1378	0.1301
		Present	**0.2114**	**0.1809**	**0.1639**	**0.1379**	**0.1305**
	(1,2)	(R. Bennai, 2019)	0.4661	0.4042	0.3677	0.3047	0.2812
		(Hosseini-Hashemi, 2011)	0.4623	0.3989	0.3607	0.2980	0.2771
		Present	**0.4628**	**0.3989**	**0.3608**	**0.2989**	**0.2779**
	(2,2)	(R. Bennai, 2019)	0.6760	0.5893	0.5365	0.4381	0.4009
		(Hosseini-Hashemi, 2011)	0.6688	0.5803	0.5254	0.4284	0.3948
		Present	**0.6688**	**0.5803**	**0.5254**	**0.4284**	**0.3948**
10	(1,1)	(R. Bennai, 2019)	0.0578	0.0494	0.0449	0.0389	0.0368
		(Hosseini-Hashemi, 2011)	0.0577	0.0490	0.0442	0.0381	0.0364
		Present	**0.0579**	**0.0498**	**0.0448**	**0.0389**	**0.0369**
	(1,2)	(R. Bennai, 2019)	0.1381	0.1184	0.1077	0.0923	0.0868
		(Hosseini-Hashemi, 2011)	0.1377	0.1174	0.1059	0.0903	0.0856
		Present	**0.1378**	**0.1177**	**0.1059**	**0.0904**	**0.0857**
	(2,2)	(R. Bennai, 2019)	0.2122	0.1825	0.1659	0.1409	0.1318
		(Hosseini-Hashemi, 2011)	0.2113	0.1807	0.1631	0.1378	0.1301
		Present	**0.2116**	**0.1808**	**0.1631**	**0.1379**	**0.1309**

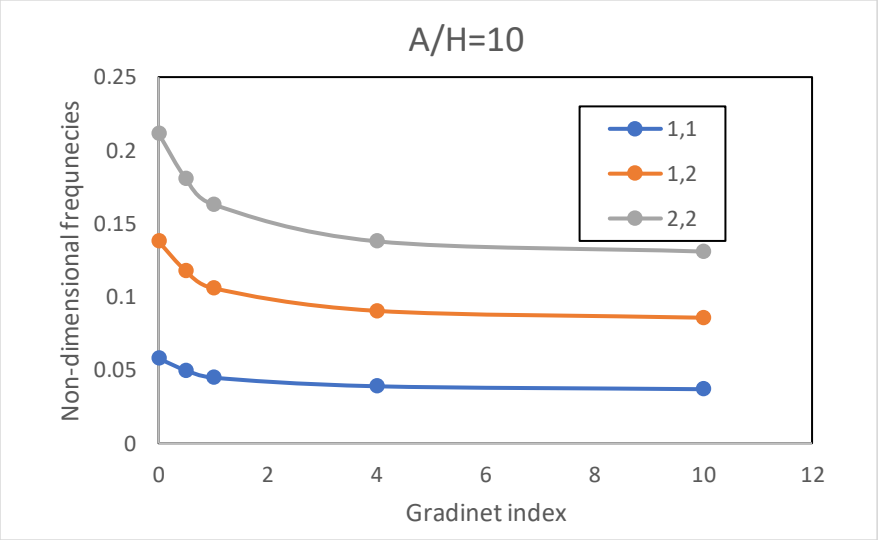

Figure IV. 1 : Effect of Gradient Indexes and Width-to-Thickness Ratios on Non-Dimensional Frequencies for Ideal Al/Al₂O₃

IV.3.3 Example 2 :

In order to verify the approach and demonstrate how porosity affects an Al/Al_2O_3 plate's frequency, a comparison of non-dimensional frequencies with (Kumar, 2023) study is made, taking into account both even and uneven porosity distributions. Selections are made for porosity levels (λ_0=0, 0.2, 0.4), width-to-thickness ratios (a/h=5, 10) and gradient indexes (p=0, 0.5, 1). The non-dimensional frequency ($\overline{w} = wh\sqrt{\rho_m/E_m}$) is consistent with material characteristics that have been documented in the literature. With a maximum error of 0.7%, the computed results in the table closely resemble those in the literature. The reason for this disparity is that, although the theory used in this study uses $K_s = \sqrt{\pi^2/12}$, (Kumar, 2023) uses $K_s = 5/6$.

Table Ⅳ. 3 : Data comparison of non-dimensional frequency of porous FGM plates.

a/h	Porosity	Theory	Gradient index p and porosity distribution					
			p=0		p=0.5		p=1	
			Even	Uneven	Even	Uneven	Even	Uneven
5	0	(Kumar, 2023)	0.4178	0.4178	0.3568	0.3568	0.3223	0.3223
		Present	**0.4151**	**0.4151**	**0.3579**	**0.3579**	**0.3248**	**0.3248**
	0.2	(Kumar, 2023)	0.4309	0.4289	0.356	0.3546	0.3066	0.3248
		Present	**0.4176**	**0.4151**	**0.3474**	**0.3540**	**0.3003**	**0.3166**
	0.4	(Kumar, 2023)	0.4500	0.4418	0.3528	0.3719	0.2681	0.3269
		Present	**0.4360**	**0.4266**	**0.3447**	**0.3610**	**0.2648**	**0.3178**
10	0	(Kumar, 2023)	0.1136	0.1136	0.964	0.0964	0.0870	0.0870
		Present	**0.1109**	**0.1109**	**0.0963**	**0.0945**	**0.0855**	**0.0855**
	0.2	(Kumar, 2023)	0.1171	0.1169	0.0961	0.0986	0.0824	0.0878
		Present	**0.1144**	**0.1141**	**0.0942**	**0.0966**	**0.0812**	**0.0863**
	0.4	(Kumar, 2023)	0.1223	0.1207	0.0949	0.101	0.0714	0.0886
		Present	**0.1194**	**0.1177**	**0.0931**	**0.0989**	**0.0708**	**0.0871**

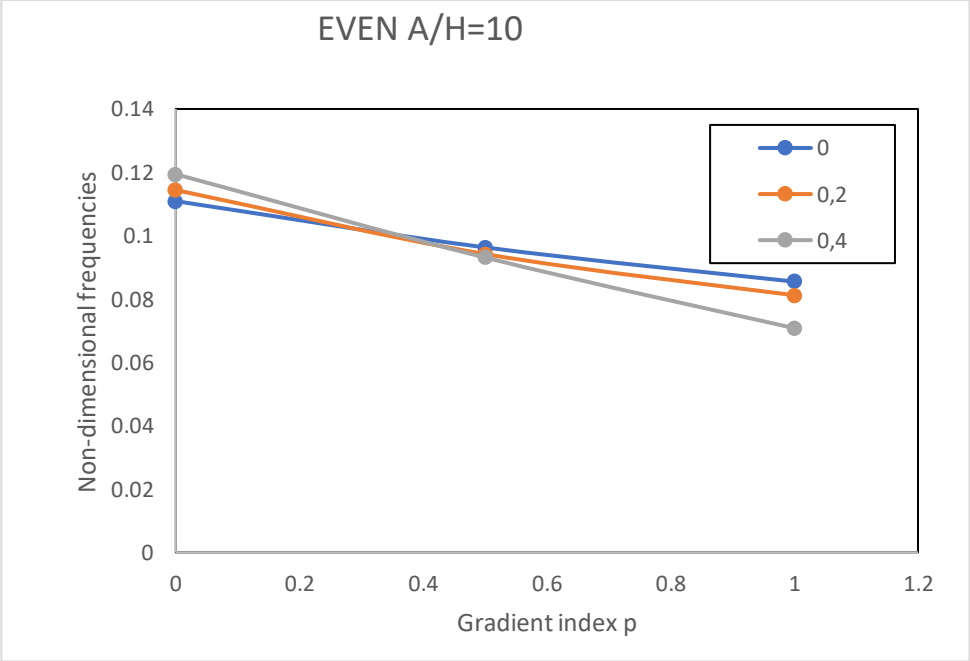

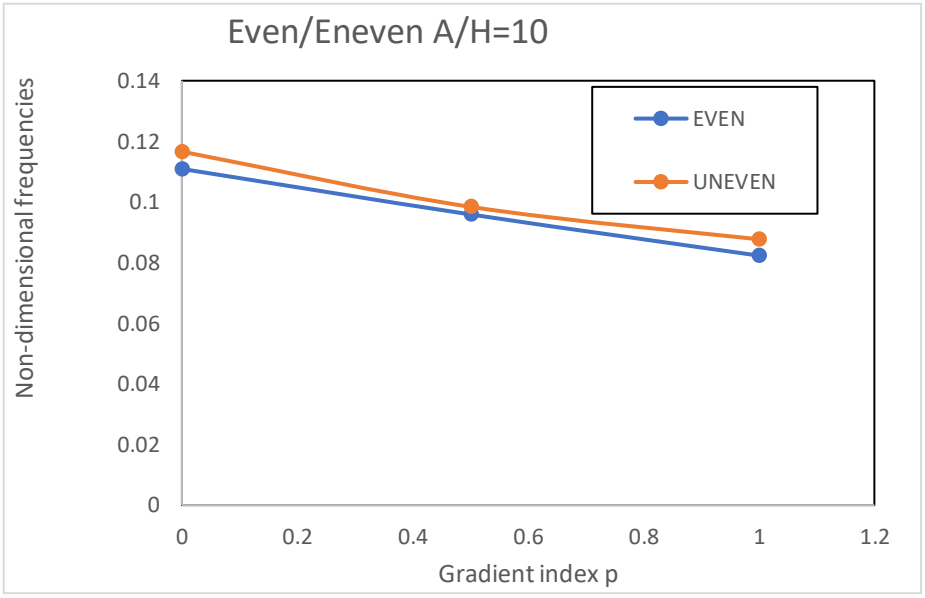

Figure Ⅳ.2: Effect of porosity on Al_2O_3 plate frequency under even and uneven distribution.

In this section, we discuss how different porosity and gradient indexes influence the non-dimensional frequency of functionally graded material (FGM) plates. Four types of distribution (type A, B, C, and D), three gradient indexes (p=0,0,5,1), and four porosities (p=0,0.2,0,4) are taken into account. Additionally, a fixed aspect ratio of a/b=1 and a width-to-thickness ratio of a/h=10 is used. The non-dimensional frequencies of the FGM plates are illustrated in the figure as affected by variations in porosity and gradient

As we observed through graphical comparison, the distribution of pores will impact the fluctuation of the vibration frequency of the FGM plate according to the porosity and gradient index. In the four porosity distributions, the frequency of P_FGM and E_FGM plates with different porosities, influenced by the change in gradient index, is identical. The frequency values increase as porosity decreases, while the higher the porosity, the lower the frequency. Similarly, as the gradient index increases, the frequency decreases, because both the presence of porosity and the reduction in the ceramic volume fraction reduce the overall stiffness of the structure.

Nevertheless, for S_FGM plates with p=0, porosity is not influenced by type A distributions, but the frequency decreases as porosity increases for p≥1. The frequency of the S_FGM plate is higher in type B distributions for higher porosity at p≥1, and decreases with increasing porosity when p≥2. The frequency decreases with increasing porosity in type C distributions, without being affected by the gradient index. Porosity influences frequency in type D distributions similarly to type C. Regardless of the grading pattern, the influence of the gradient index on FGM plates is similar.

IV.4 Effect of width-to-thickness ratio :

To Investigate If Different Porosity Distributions Affect How the Width-To-Thickness Ratio Affects Frequency, Table 4 Provides the Corresponding Values for Porous FGM plates With Different Width-To-Thickness Ratios Under Unequal Distributions($\boldsymbol{a/h}$=5, 10, 15, 20) are fixed, and porosity$\boldsymbol{\lambda_0 = 0,3}$

The results show that regardless of the kind of porosity distribution, when the width-to-Thickness ratio rises, the frequency decreases given the aspect ratio, gradient index, and porosity .this is the consequence of the thinner thickness of the plate causing a decrease in rigidity. Additionally, when a/h>10, we found that the trend is continuously changing and that the difference in frequencies impacted by the gradient index is not immediately obvious. This leads to a simple influence rule, which is most noticeable in S-FGM.

Table IV. 4: Effect of width-to-thickness ration on the non-dimensional frequency of porous P, E, S-FGM plates under type B, C and, D distribution.

Pattern	Gradient Index	Width-to-thickness and porosity distribution											
		Type B				Type C				Type D			
		$a/h=5$	$a/h=10$	$a/h=15$	$a/h=20$	$a/h=5$	$a/h=10$	$a/h=15$	$a/h=20$	$a/h=5$	$a/h=10$	$a/h=15$	$a/h=20$
P-FGM	P=0	0.4263	0.1172	0.0532	0.0301	0.4106	0.112	0.0507	0.0287	0.0481	0.1145	0.0519	0.0294
	P=1	0.322	0.0878	0.0397	0.0225	0.2935	0.0789	0.0356	0.0201	0.2902	0.0780	0.0352	0.0199
	P=2	0.2837	0.0775	0.0351	0.0199	0.2477	0.0665	0.03	0.017	0.234	0.0626	0.0282	0.0160
	P=3	0.2689	0.0739	0.0335	0.019	0.2296	0.0618	0.0279	0.0158	0.2095	0.0561	0.0253	0.0143
	P=4	0.2621	0.0724	0.0329	0.0186	0.2215	0.0598	0.027	0.0153	0.1982	0.0532	0.0240	0.0136
	P=5	0.2582	0.0716	0.0326	0.0185	0.2171	0.0588	0.0266	0.015	0.1927	0.0518	0.0234	0.0132
E-FGM	P=0	0.4263	0.1172	0.0532	0.0301	0.0301	0.4106	0.112	0.0507	0.4181	0.0870	0.0519	0.0294
	P=1	0.2911	0.0796	0.0361	0.0204	0.0204	0.2587	0.0696	0.0314	0.2499	0.0855	0.0303	0.0171
	P=2	0.265	0.0729	0.0331	0.0188	0.0188	0.2267	0.0611	0.0276	0.2085	0.0824	0.0252	0.0143
	P=3	0.2559	0.0709	0.0323	0.0183	0.0183	0.2157	0.0583	0.0263	0.1940	0.0812	0.0235	0.0133
	P=4	0.2512	0.07	0.0319	0.0181	0.0181	0.2102	0.057	0.0258	0.1879	0.0714	0.0228	0.0129
	P=5	0.2479	0.0694	0.0316	0.018	0.018	0.2065	0.0561	0.0254	0.1847	0.0708	0.0225	0.0127
S-FGM	P=0	0.3532	0.0974	0.0441	0.025	0.3295	0.0897	0.0406	0.023	0.0304	0.0931	0.0422	0239
	P=1	0.322	0.0878	0.0397	0.0225	0.2935	0.0789	0.0356	0.0201	0.2902	0.0780	0.0352	0.0199
	P=2	0.302	0.0818	0.037	0.0209	0.2698	0.0721	0.0325	0.0184	0.2611	0.0696	0.0314	0.0177
	P=3	0.292	0.0789	0.0356	0.0202	0.2578	0.0686	0.0309	0.0175	0.2464	0.0654	0.0294	0.0166
	P=4	0.2865	0.0772	0.0349	0.0197	0.2512	0.0668	0.03	0.017	0.2381	0.0631	0.0284	0.0160
	P=5	0.2832	0.0763	0.0344	0.0195	0.2471	0.0656	0.0295	0.0167	0.2331	0.0617	0.0278	0.0157

IV.5 Effect of porosity distribution:

This section explores the influence of different porosity distributions on the non-dimensional frequency of porous functionally graded plates. The study assumes consistent default settings. Figure Ⅱ.3 type B- C-D illustrate the variations in the effects of various porosity distributions on the non-dimensional frequencies of functionally graded plates with three grading patterns.

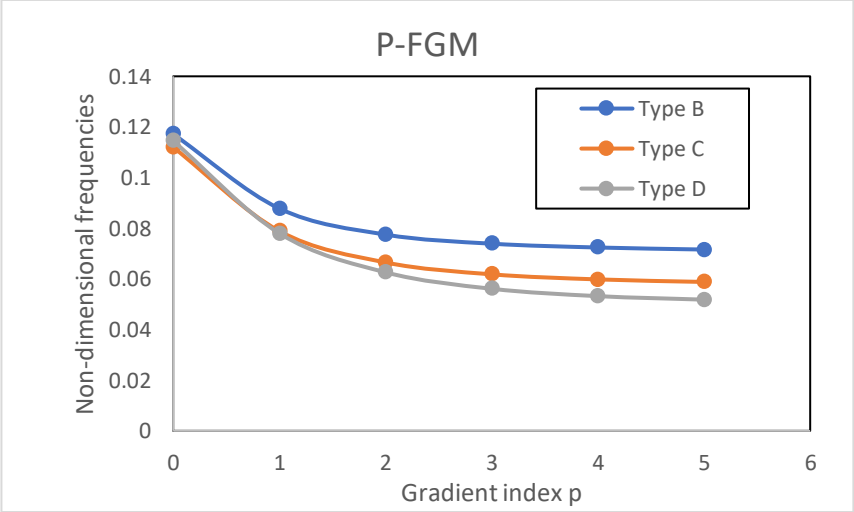

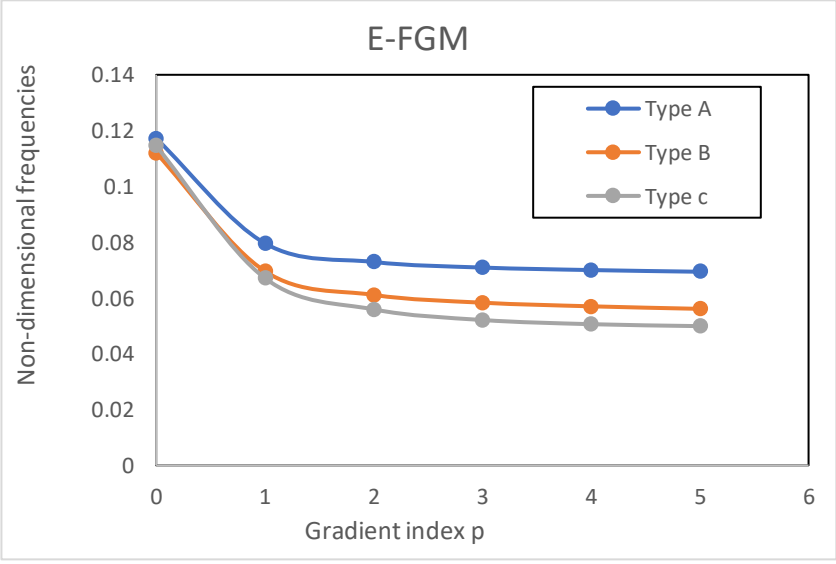

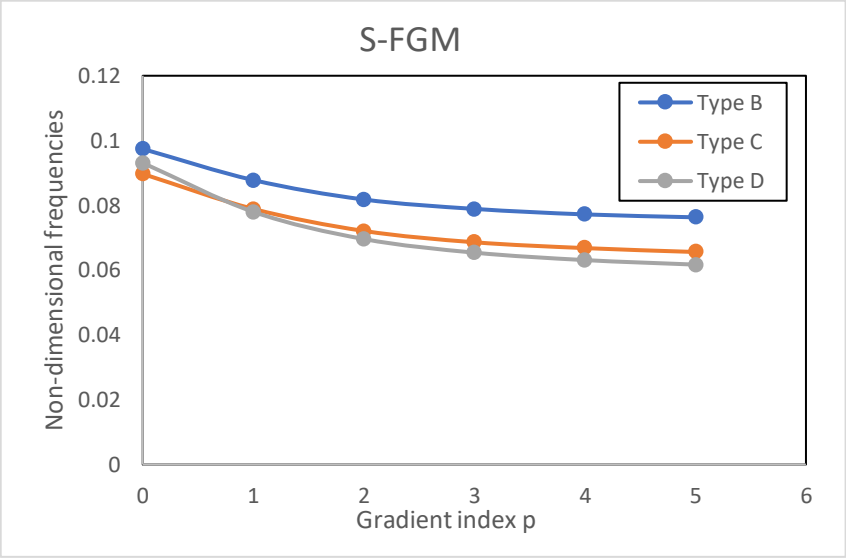

Figure IV.3: Effect of distribution type on the frequency value of P, E, S-FGM plates.

In terms of P-FGM, E-FGM and S-FGM , the non-dimensional frequency satisfies type B> type D> type C for p=0,and type B> type C> type D for p=1>.at greater gradient index, the frequencies of type B, type C, type D are increased by approximate.

We found that, regardless of the grading scheme, the frequency under a uniform porosity distribution is always smaller than the three other uneven porosity distributions when p1.the increase in frequency under an uneven porosity distribution compared to a uniform porosity distribution is most significant in E-FGMs. conversely; the frequency increase of S-FGMs under an uneven distribution is the smallest.

IV.6 Effect of ceramic material:

Table Ⅳ 5 includes a list of the frequency values corresponding to the B-type, C-type, and D-type porosity distributions. We discovered that for the three ceramic compositions with irregular porosity distribution, the difference between P-FGM and E-FGM frequency growth develops with increasing gradation index deceases. The porosity distribution and gradient index will have an inverse trend of influence on the vibration performance of P-FGM and E-FGM plates made of different ceramic materials. For S-FGM plates composed of three different ceramic materials, the previously indicated effects are negligible, they all show significant frequency fluctuations with different porosity distributions.

Table IV 5: Effect of ceramic material on the non-dimensional frequency of porous P, E, S-FGM Plates under type B C and D distributions.

Pattern	Gradient index	**Ceramic material and porosity distribution**								
		Type B			**Type C**			**Type D**		
		A12O3	SiC	Si3N4	A12O3	SiC	Si3N4	A12O3	SiC	Si3N4
P-FGM	P=0	0.4263	0.4413	0.5488	0.4106	0.4248	0.5292	0.4181	0.4327	0.5386
	P=1	0.322	0.3243	0.363	0.2935	0.2967	0.3308	0.2902	0.2944	0.3268
	P=2	0.2837	0.2862	0.3052	0.2477	0.253	0.2664	0.234	0.2428	0.2513
	P=3	0.2689	0.2715	0.2826	0.2296	0.2364	0.2412	0.2095	0.2222	0.2198
	P=4	0.2621	0.2643	0.2716	0.2215	0.2286	0.2295	0.1982	0.2130	0.2052
	P=5	0.2582	0.2599	0.265	0.2171	0.224	0.2228	0.1927	0.2082	0.1976
E-FGM	P=0	0.4263	0.4413	0.5489	0.4106	0.4248	0.5292	0.4181	0.4327	0.5386
	P=1	0.2911	0.298	0.3265	0.2587	0.2675	0.2902	0.2499	0.2613	0.2800
	P=2	0.265	0.2703	0.284	0.2267	0.2358	0.2429	0.2085	0.2233	0.2231
	P=3	0.2559	0.2601	0.2682	0.2157	0.2244	0.2259	0.194	0.2103	0.2030
	P=4	0.2512	0.2544	0.2597	0.2102	0.2183	0.2172	0.1879	0.2044	0.1940
	P=5	0.2479	0.2503	0.254	0.2065	0.2141	0.2115	0.1847	0.2010	0.1891
S-FGM	P=0	0.3532	0.3519	0.3994	0.3295	0.3283	0.3726	0.3404	0.3391	0.3849
	P=1	0.322	0.3243	0.363	0.2935	0.2967	0.3308	0.2902	0.2943	0.3268
	P=2	0.302	0.3071	0.3398	0.2698	0.2764	0.3036	0.2611	0.2694	0.2935
	P=3	0.292	0.2986	0.3283	0.2578	0.2662	0.2898	0.2464	0.2570	0.2767
	P=4	0.2865	0.2939	0.322	0.2512	0.2607	0.2822	0.2381	0.2502	0.2673
	P=5	0.2832	0.2911	0.3182	0.2471	0.2573	0.2776	0.2331	0.2461	0.2616

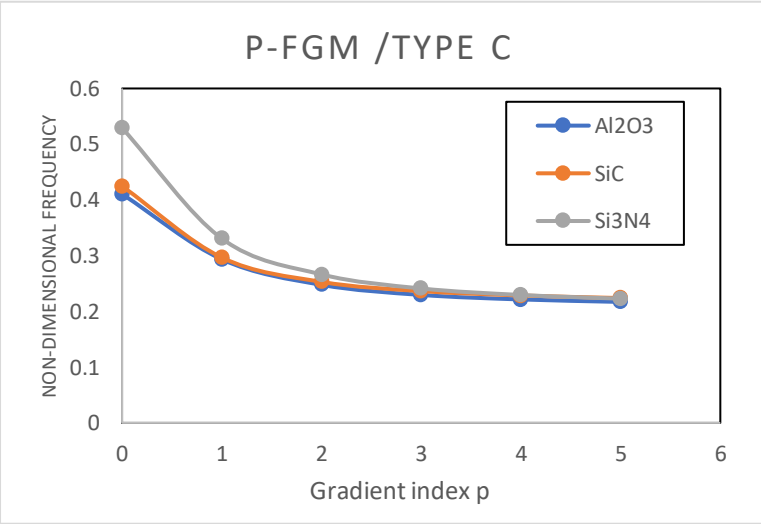
P-FGM /TYPE C
NON-DIMENSIONAL FREQUENCY
0.6
0.5
0.4
0.3
0.2
0.1
0
0
1
2
3
4
5
6
Gradient index p
Al2O3
SiC
Si3N4

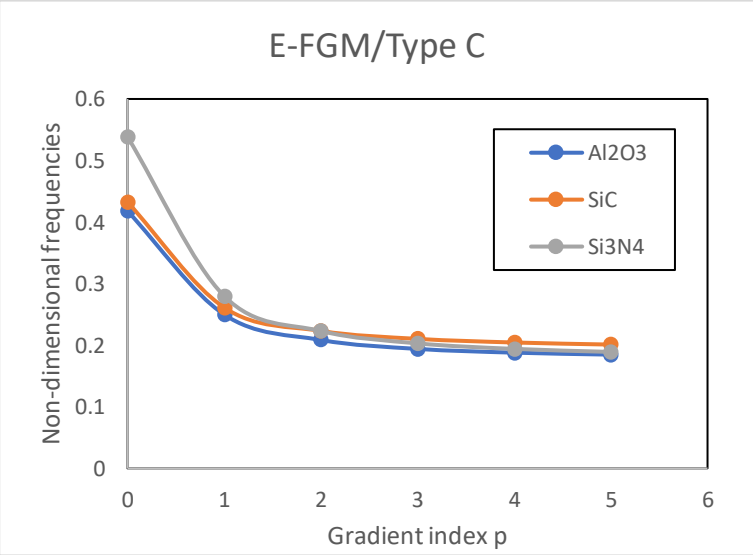
E-FGM/Type C
Non-dimensional frequencies
0.6
0.5
0.4
0.3
0.2
0.1
0
0
1
2
3
4
5
6
Gradient index p
Al2O3
SiC
Si3N4

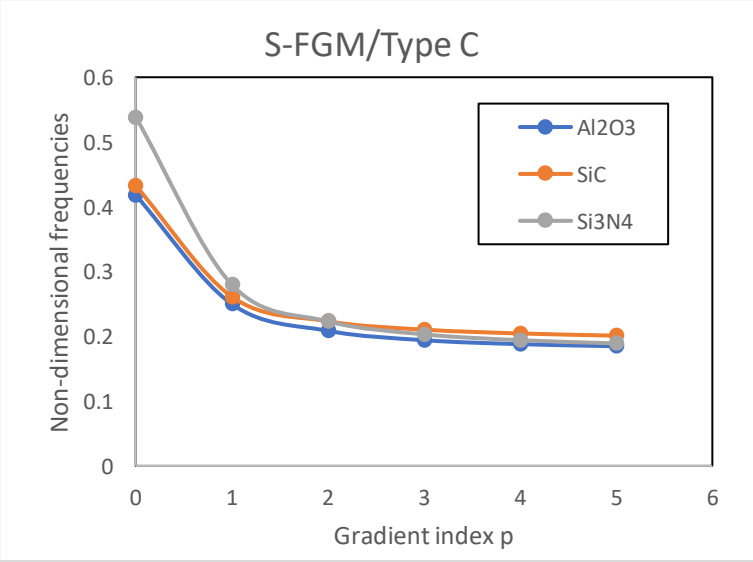
S-FGM/Type C
Non-dimensional frequencies
0.6
0.5
0.4
0.3
0.2
0.1
0
0
1
2
3
4
5
6
Gradient index p
Al2O3
SiC
Si3N4

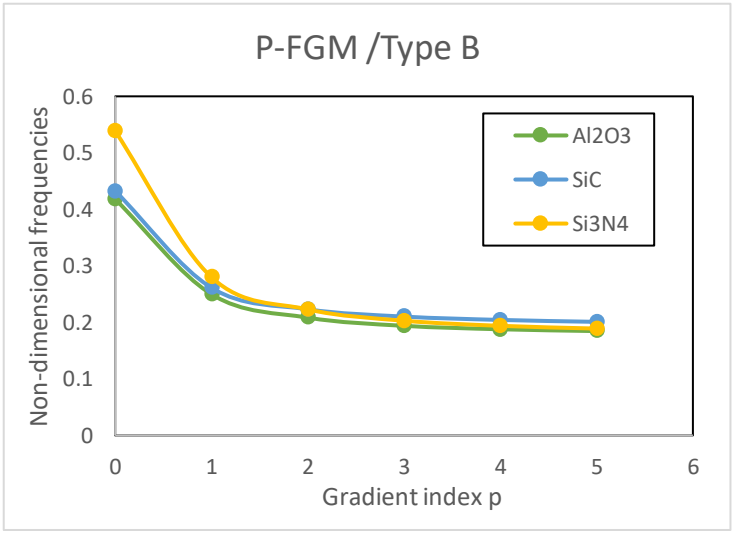
P-FGM /Type B
Non-dimensional frequencies
0.6
0.5
0.4
0.3
0.2
0.1
0
0
1
2
3
4
5
6
Gradient index p
Al2O3
SiC
Si3N4

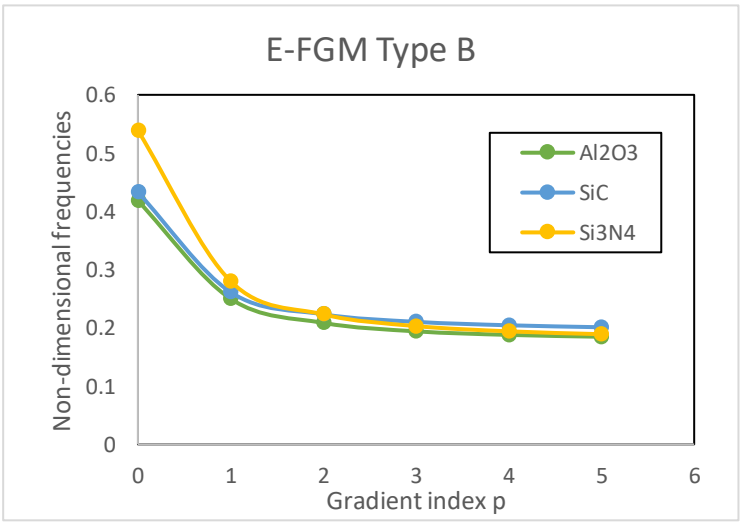
E-FGM Type B
Non-dimensional frequencies
0.6
0.5
0.4
0.3
0.2
0.1
0
0
1
2
3
4
5
6
Gradient index p
Al2O3
SiC
Si3N4

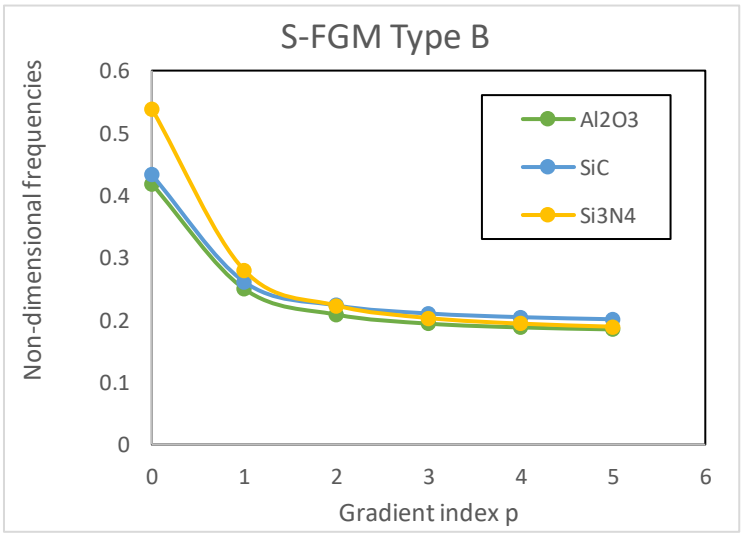
S-FGM Type B
Non-dimensional frequencies
0.6
0.5
0.4
0.3
0.2
0.1
0
0
1
2
3
4
5
6
Gradient index p
Al2O3
SiC
Si3N4

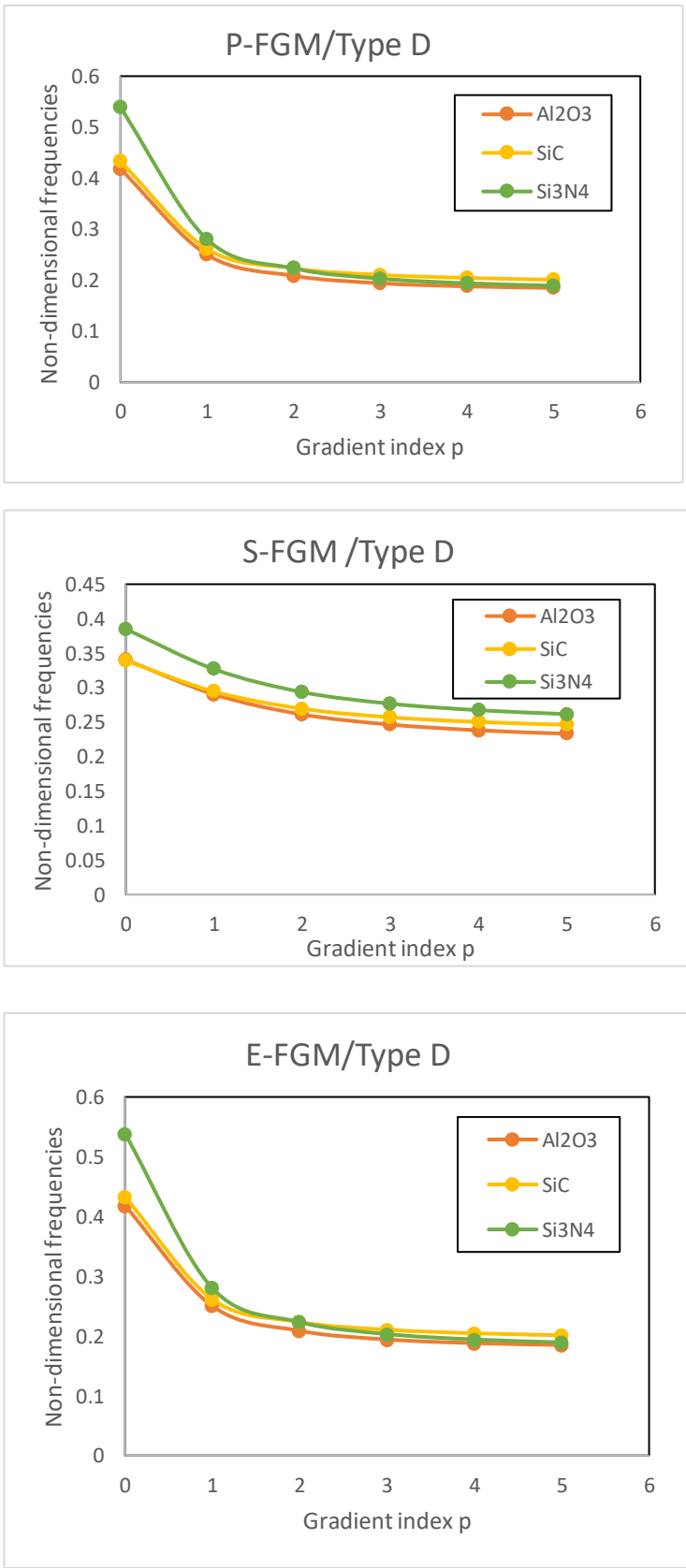

Figure IV.4: Effect of ceramic material of ceramic material on the frequency value of P, E, S-FGM plate under type B, C, D.

The non-dimensional frequency of porous FGM plates is examined in this section along with how plate settings are modified based on the preceding section.figs.9$(B), (C), (D)$. display the frequency fluctuation made up of three distinct material groups $(AL/AL_2O_3)(AL/SiC)$ (AL/Si_3N_4) .

IV.7 Effect of grading pattern :

Using the study presented above, this section mainly highlights the effects of different grading patterns on the non-dimensional frequency of porous FGM plates. Figure5.type B, C, D, show the comparison of frequency values of FGM plates with different grading patterns, taking into account different porosity distributions.it has been observed that the gradient index influences the frequencies of porous FGM plates in a similar way for all three grading patterns. The frequency difference values always satisfy S-FGM >P-FGM> E-FGM as the gradient index rises. Since varied grading patterns are present, the frequency is most noticeable in uniform porosity distribution. With p=5, the frequency of S-FGM increases by approximate compared to P-FGM /E-FGM.

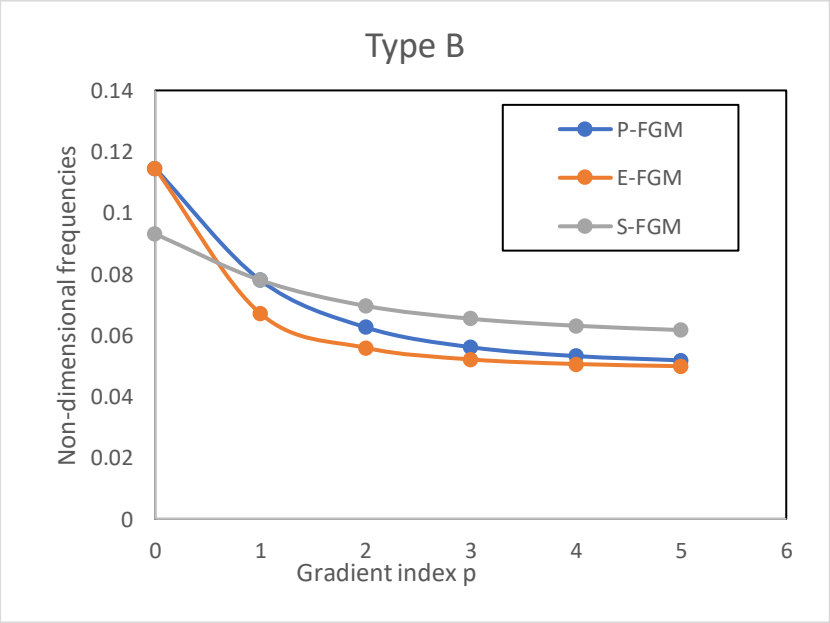

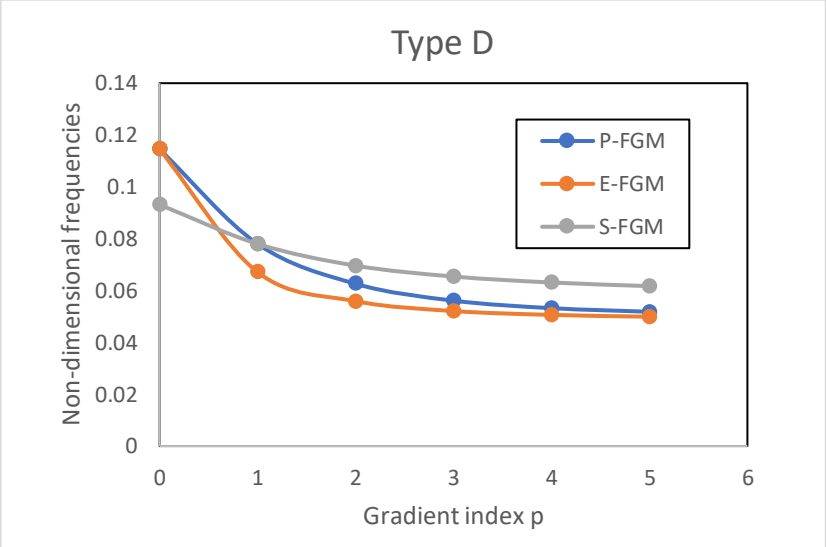

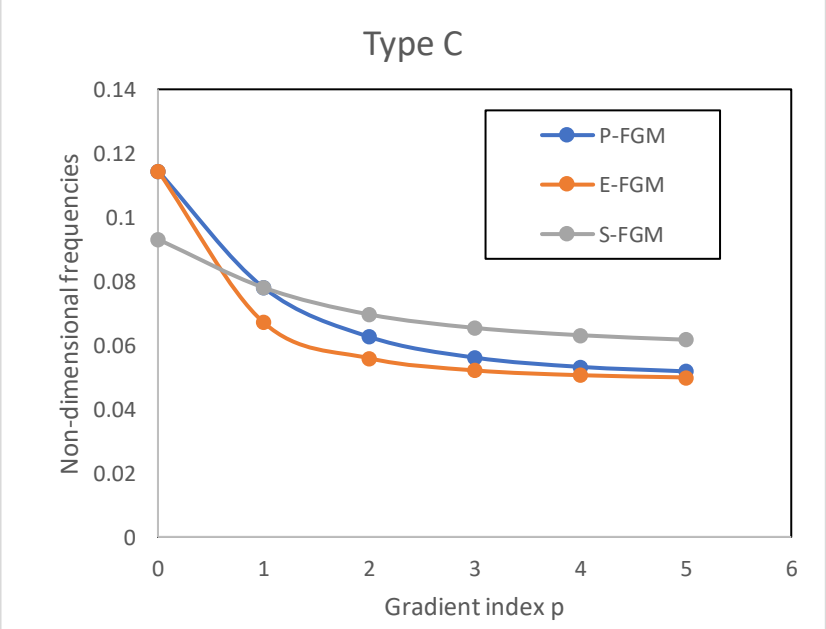

Figure. IV 5: Effect of grading pattern on the frequency value under type B, C, D distribution.

IV.7 Conclusion:

In the first part of this chapter, we presented the results of the free vibration analysis of FGM plates using the first order shear deformation theory (FSDT).

Second, we studied the effect of the porosity of an FGM plate on the deflection, normal and transverse shear stresses through its thickness.it turns out that porosity influences the mechanical responses in bending of the FGM plate and that it is important to consider this parameter in the study of stability.

All comparative studies have shown that the results deformation theories are nearly identical.

Therefore, it can be said that the proposed theory is simple and effective for analyzing the free vibration of functionally graded plates with different porosity.

General Conclusion

The application of Hamilton's principle and the Navier technique made it possible to precisely derive the motion equations for porous FGM plates, which made it easier to conduct a thorough examination of their dynamic response. Comparisons with multiple cases validated the accuracy and robustness of our analytical approach, laying a solid basis for future work in this field. The complex interactions between gradation models, porosity distribution, and the mechanical behavior of FGMs have been clarified by this work, opening new avenues for material design and technical applications. Furthermore, our results highlight how FGMs can improve structural performance and efficiency in a variety of industries, spurring innovation and sustainability.

The application of the Navier method and the Hamilton principle allowed for the precise derivation of the movement equations for the FGM porous plaques, enabling a thorough analysis of their dynamic response. The comparison with multiple examples confirms the accuracy and reliability of our analytical method, providing a strong foundation for further research in this area. These findings open up new avenues for the study and improvement of the behavior of FGM materials as well as for their use in various fields of engineering and technology.

Our comparative analysis of the key parameters has led to several significant findings:

- The distribution of porosity of type B indicates the least significant impact of the gradient index, whereas increases in porosity, the gradient index, and the ratio width/thickness cause a decrease in the non-dimensional frequency.

- In particular, higher gradient indices are typically associated with smaller frequency values in a uniform porosity distribution compared to an uneven distribution.

- The choice of porosity distribution has a significant impact on frequency improvement; uniform distribution results in the most significant improvement for E-FGM plaques.

- The influence of the gradient index on non-dimensional frequencies varies according on the gradation models and ceramic materials, highlighting the complexity of FGM behavior.

- Notably, there are significant frequency differences observed in a uniform porosity distribution, with the S-FGM plaques showing the strongest increase with increasing

gradient index.

Furthermore, our optimization approach, which incorporates the choice of metallic and ceramic materials as concept-related variables, aims to identify the most efficient metal-ceramic combination to achieve optimization goals like mass and cost minimization. This approach demonstrates how FGM can enhance structural concepts in civil engineering applications, resulting in more resilient and effective infrastructures.

Taking into consideration a variety of factors, including durability, resistance, and profitability, our optimization approach seeks to determine the appropriate balance between the constituent materials for any particular application. With the use of advanced analytical tools and optimization approaches, we are able to predict and model the behavior of FGM structures under various environmental stresses and circumstances.

In addition to ensuring good long-term performance, the practical adoption of this approach may result in significant material and manufacturing cost savings. Engineers may design more resilient and effective infrastructures and contribute to a sustainable and prosperous future by investing in the research and development of FGM materials and utilizing advanced optimization methodologies.

Finally, our optimization approach demonstrates the potential of FGM to change conception and construction practices in the field of civil engineering. By including advanced material considerations into the conceptualization process, we will pave the way for more resilient and effective infrastructures that can adapt to the changing needs of our ever-changing society.

Bibliography

ABDELBARI, S. (2016). Etude des structures à section en matériaux a gradient évalué FGM. (Doctoral dissertation).

ABDELHAK, Z. (2016). Analyse et modélisation du comportement des plaques en matériaux à gradient de propriétés type FGM sous chargement thermomécanique. (Doctoral dissertation).

Abdelouahed Tounsi, E. A. (2013). Mathematical Modeling and Optimization of Functionally Graded Structures. *Mathematical Problems in Engineering*.

Abrate, S. (2008). Functionally graded plates behave like homogeneous plates. *Composites part B: engineering*, 39(1), 151-158.

Afaq, K. S. (2003). Développement d'un nouveau modèle pour les structures Composites multicouches et sandwichs avec prise en compte du cisaillement transverse et des effets de bord. *thèse de doctorat*. Université Toulouse III - Paul Sabatier, France: thèse de doctorat.

AIT FERHAT, Y. (2021, juin 3). ÉTUDE NUMERIQUE DU COMPORTEMENT EN RUPTURE DES MATERIAUX EN FGM SOUS DIFFERENTS TYPES DE CHARGEMENT. sidi bel abbes, Génie Mécanique, Algérie.

Ambartsumyan, S. A. (1969). *« Theory of anisotropic plate ».* Technomic Publishing Co.

Anh, V. T. (2021). Nonlinear dynamic analysis of porous graphene platelet-reinforced composite sandwich shallow spherical shells. *Mechanics of Composite Materials*, 57, 609-622.

Aydogdu, M. &. (2007). Free vibration analysis of functionally graded beams with simply supported edges. *Materials & design*, 28(5), 1651-1656.

Aydogdu, M. (2005). Vibration analysis of cross-ply laminated beams with general boundary conditions by Ritz method. *International Journal of Mechanical Sciences*, 1740-1755.

Belkacem, A. (2015). Etude de la stabilité des plaques en matériaux composites: analyse et modélisation. FACULTE DES SCIENCES APPLIQUEES: Doctoral dissertation.

BENBAKHTI A, D. (2017). Modélisation du comportement thermomécanique des plaques FGM (Functionally Graded Materials). Université de Mostaganem-Abdelhamid Ibn Badis: (Doctoral dissertation).

BOUAMAMA, M. (2019). Etude du comportement dynamique et stabilité des poutres en FGM. Génie Mécanique, Algerie.

BOUKHARI, A. (2016). Application des théories à ordre élevé de déformation de cisaillement pour l'étude du comportement mécanique des plaques épaisses. (Doctoral dissertation).

BRAIRI, S. (2019, 4 20). ANALYSE DE LA DÉGRADATION DES STRUCTURES FGM RENFORCÉES PAR FRP PRÉCONTRAINTS. Tlemcen, GÈnie MÈcanique , Algerie.

C. M. C. Roque, A. J. (2007). A radial basis function approach for the free vibration analysis of fuctionnally graded plates using a refined. *Journal of Sound and vibration*, 300 (3-5) 1048-1070.

Chi, S. H. (2003). Cracking in coating–substrate composites with multi-layered and FGM coatings. *Engineering Fracture Mechanics*, 70(10), 1227-1243.

Chikh, A. (2019). Analysis of static behavior of a P-FGM Beam. . *Journal of Materials and Engineering Structures«JMES»*, 6(4), 513-524.

Cuong-Le, T. N.-L.-T.-V. (2022). Nonlocal strain gradient IGA numerical solution for static bending, free vibration and buckling of sigmoid FG sandwich nanoplate. *Physica B: Condensed Matter*, 631, 413726.

Delale, F. &. (1983). The crack problem for a nonhomogeneous plane. *.ASME Journal of Applied Mechanics*, 50 (3): 609-614,.

E. Reissner, Y. S. (1961). Bending and Stretching of Certain Types of Heterogeneous Aeolotropic Elastic Plates. *Journal of Applied Mechanics* .

Functionally Graded Materials (FGM) and Their Production Methods. (2002, August 22). Récupéré sur Azom.com.

Gay, D. (2022). *Composite materials: design and applications.* CRC press.

Guellil, M. k. (2022, janvier 6). Étude de comportement mécanique des plaques fgm reposant sur des fondations élastiques sous diverses conditions aux limites. sidi bel abbes , Génie Civil, Algérie.

Guellil, M. S.-Z. (2021). Influences of porosity distributions and boundary conditions on mechanical bending response of functionally graded plates resting on Pasternak foundation. *Steel and Composite Structures*, 38(1), 1.

Harris, B. (1999). *ENGINEERING COMPOSITE MATERILAS.* LONDON: The Institute of Materials.

Hosseini-Hashemi, S. F. (2011). A new exact analytical approach for free vibration of Reissner–Mindlin functionally graded rectangular plates. *International Journal of Mechanical Sciences*, 53(1), 11-22.

Hosseini-Hashemi, S. F. (2011). Study on the free vibration of thick functionally graded rectangular plates according to a new exact closed-form procedure. *Composite Structures*, 93(2), 722-735.

Hu, X. &. (2023). Free vibration analysis of functionally graded plates with different porosity distributions and grading patterns. *ournal of Mechanical Science and Technology, 37(11)*, 5725-5738.

Hu, X. &. (2023). Free vibration analysis of functionally graded plates with different porosity distributions and grading patterns. *Journal of Mechanical Science and Technology*, 37(11), 5725-5738.

Javaheri, R. &. (2002). Buckling of functionally graded plates under in-plane compressive loading. *ZAMM-Journal of Applied Mathematics and Mechanics/Zeitschrift für Angewandte Mathematik und Mechanik: Applied Mathematics and Mechanics*, 82(4), 277-283.

Jin, Z. H. (1996). Stress intensity relaxation at the tip of an edge crack in a functionally graded material subjected to a thermal shock. *Journal of thermal stresses*, 19(4), 317-339.

Jrad, H. M. (2019). Geometrically nonlinear analysis of elastoplastic behavior of functionally graded shells. *Engineering with Computers*, 35, 833-847.

Kolvik, G. M. (2012). Higher order shear deformation plate theory. (Master's thesis).

Kumar, V. S. (2023). Vibration response analysis of tapered porous FGM plate resting on elastic foundation. *International Journal of Structural Stability and Dynamics*, 23(02), 2350024.

Leissa, A. W. (1973). The free vibration of rectangular plates. Journal of sound and vibration. 31(3), 257-293.

Liu, B. F. (2016). Analysis of functionally graded sandwich and laminated shells using a layerwise theory and a differential quadrature finite element method. *Composite Structures*, 136, 546-553.

M. Kaddari, A. K.-O. (2020). A study on the structures behavior of functionally graded porous plates on elastic foundation using a new quasi-2D model :bendin and free vibration analysis. *Computers and Concrete* , 25 (1) (2020) 37-57.

M.Koizumi. (1993). The concept of FGM. *functionally gradient materials,Cerams trans*, 34,3-10.

mahamood, r. m. (2017). *functionally graded materials.* Springer.

Mohammadi, M. S. (2010). Levy solution for buckling analysis of functionally graded rectangular plates. Applied Composite Materials. *Applied Composite Materials*, 17, 81-93. Récupéré sur https://link.springer.com/article/10.1007/s10443-009-9100-z

Murthy, M. (1981). *An improved transverse shear deformation theory for laminated.* NASA.

N.D.Duc. (2014). Nonlinear static and dynamic stability of functionally graded plates and shells. *Vietnam National University Press*, Hanoi.

Nguyen, H. N. (2019). A refined simple first-order shear deformation theory for static bending and free vibration analysis of advanced composite plates materials . 12(15), 2385.

Nguyen, H. N. (2019). A refined simple first-order shear deformation theory for static bending and free vibration analysis of advanced composite plates. *Materials*, 12(15), 2385.

Ochoa, O. O. (1992). *Finite element analysis of composite laminates.* Springer Netherlands.

Parida, S. P. (2020). Free and forced vibration analysis of flyash/graphene filled laminated composite plates using higher order shear deformation theory. Proceedings of the Institution of Mechanical Engineers, Part C. *Journal of Mechanical Engineering Science*, 236(9), 4648-4659.

R. Bennai, H. A.-O. (2019). Free vibration response of functionally graded porous plates uding a higher order shear and normal deformation theory. *Earthquakes and Structures* , 16 (5) 547-561.

Randjbaran, E. e. (2015). A review paper on comparison of numerical techniques for finding approximate solutions to boundary value problems on post-buckling in functionally graded materials. *Trends Journal of Sciences Research* .

Reddy J.N. (1999). *Theory and Analysis of Elastic plates.* Philadelphia: Taylor & Francis.

Reissner, E. (1945). *The effect of transverse shears deformation on the bending of elastic plates.*

SAID, A. (2015). Etude et analyse des plaques FGM en Génie Civil. Doctoral dissertation.

Saleh, B. J.-h. (2020). 30 Years of functionally graded materials: An overview of manufacturing methods, Applications and Future Challenges. *Composites Part B: Engineering*, 201, 108376.

SOMIYA, S. (2013). *Handbook of Advanced Ceramics:materials, applications, processing, and properties.* Academic press.

Thai, H. T. (2013). A simple first-order shear deformation theory for the bending and free vibration analysis of functionally graded plates. *Composite Structures*, 101, 332-340.

Thanh, C. L. (2020). A geometrically nonlinear size-dependent hypothesis for porous functionally graded micro-plate. *Engineering with Computers*, 1-12.

Timoshenko, S. &.-K. (1959). Theory of plates and shells . *New York: McGraw-hill*, Vol. 2, pp. 240-246.

Touratier, M. (1991). An efficient standard plate theory. *International journal of engineering science*, 901-916.

Valizadeh, N. N.-E. (2013). NURBS-based finite element analysis of functionally graded plates: static bending, vibration, buckling and flutter. *Composite Structures*, 99, 309-326.

ziou, h. (2017, 04 23). Contribution à la modélisation des structures en materiaux à gradient fonctionnele. Biskra, Génie Civil et Hydraulique, Algerie : Université Mohamed Khider.

Zu, Y. .. (2017). Large amplitude vibration of sigmoid functionally graded thin plates with porosities . *Thin Walled Structurs* , 119 911-924.